



A re-evaluation of the Meso-Cenozoic thermo-tectonic evolution of Bogda Shan (Tian Shan, NW China) based on new basement and detrital apatite fission track thermochronology

Zhiyuan He, Stijn Glorie, Fujun Wang, Wenbin Zhu, Ana Fonseca, Wenbo Su, Linglin Zhong, Xin Zhu & Johan De Grave

To cite this article: Zhiyuan He, Stijn Glorie, Fujun Wang, Wenbin Zhu, Ana Fonseca, Wenbo Su, Linglin Zhong, Xin Zhu & Johan De Grave (2023) A re-evaluation of the Meso-Cenozoic thermo-tectonic evolution of Bogda Shan (Tian Shan, NW China) based on new basement and detrital apatite fission track thermochronology, International Geology Review, 65:13, 2093-2112, DOI: [10.1080/00206814.2022.2121946](https://doi.org/10.1080/00206814.2022.2121946)

To link to this article: <https://doi.org/10.1080/00206814.2022.2121946>



[View supplementary material](#)



Published online: 08 Sep 2022.



[Submit your article to this journal](#)



Article views: 454



[View related articles](#)



[View Crossmark data](#)



Citing articles: 11 [View citing articles](#)

A re-evaluation of the Meso-Cenozoic thermo-tectonic evolution of Bogda Shan (Tian Shan, NW China) based on new basement and detrital apatite fission track thermochronology

Zhiyuan He ^a, Stijn Glorie^b, Fujun Wang^c, Wenbin Zhu^c, Ana Fonseca^a, Wenbo Su^a, Linglin Zhong^d, Xin Zhu^e and Johan De Grave^a

^aLaboratory for Mineralogy and Petrology, Department of Geology, Ghent University, Krijgslaan 281 S8, 9000, Ghent, Belgium; ^bDepartment of Earth Sciences, School of Physical Sciences, The University of Adelaide, SA-5005, Adelaide, SA, Australia; ^cState Key Laboratory for Mineral Deposits Research, School of Earth Sciences and Engineering, Nanjing University, 210023 Nanjing, China; ^dCollege of Earth Sciences, Chengdu University of Technology, Chengdu 610059, China; ^eState Key Laboratory of Continental Dynamics, Department of Geology, Northwest University, 710069 Xi'an, China

ABSTRACT

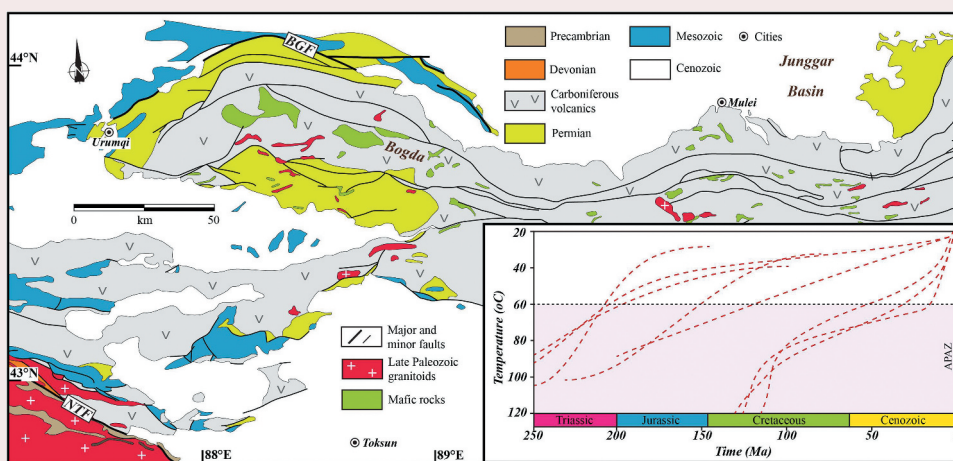
Bogda Shan is a mountain belt located at the eastern extremity of the Chinese Tianshan and records a complex and debated exhumation history. Previous studies have reported a young Cenozoic thermal history for the exhumation of Bogda Shan, which is in conflict with the observation of preserved Mesozoic erosion surfaces in the area. This study re-evaluates the Meso-Cenozoic thermo-tectonic evolution of Bogda Shan using apatite fission track (AFT) thermochronology. Palaeozoic basement (meta-sandstone) samples collected from the northern and southwestern flanks of the mountain ranges reveal apparent Mesozoic AFT ages ranging from ~202 Ma to ~97 Ma. Inverse thermal history modelling results reveal slow to moderate basement cooling during the early Mesozoic, corresponding to relatively low levels of exhumation. This accounts for the preservation of low-relief Mesozoic peneplanation surfaces recognized at elevations of ~3500–4000 m. None of the presented AFT data and thermal history models show any evidence for significant deep Cenozoic exhumation. In the neighbouring Junggar Basin, a Middle Jurassic sandstone sample records partial resetting of the AFT system during the Cretaceous. This observation conflicts with previous data (from the same Jurassic strata) where complete resetting of the AFT clock during the Cenozoic was suggested. Furthermore, Lower Cretaceous and Palaeogene sediments from the Turpan-Hami Basin show non-reset detrital AFT age populations of ~197, ~135, and ~104 Ma, which are coincident with the main pulses of exhumation recorded in the Chinese North Tianshan. Based on a comprehensive summary of the published data, we argue for a Mesozoic building of the Bogda–Balikun–Harlik mountain chain in the eastern Chinese Tianshan. Subsequent Cenozoic exhumation must have been relatively modest at most (<2 km) as it was not recorded by AFT thermochronology.

ARTICLE HISTORY

Received 26 June 2022
Revised 28 August 2022
Accepted 3 September 2022

KEY WORDS

Tian Shan; apatite fission track thermochronology; peneplanation surface; Intra-continental deformation



CONTACT Zhiyuan He  Zhiyuan.He@UGent.be  Laboratory for Mineralogy and Petrology, Department of Geology, Ghent University, Krijgslaan 281 S8, 9000, Ghent, Belgium; Wenbin Zhu  wzb@nju.edu.cn  State Key Laboratory for Mineral Deposits Research, School of Earth Sciences and Engineering, Nanjing University, 210023 Nanjing, China

 Supplemental data for this article can be accessed online at <https://doi.org/10.1080/00206814.2022.2121946>.

© 2022 Informa UK Limited, trading as Taylor & Francis Group

1. Introduction

The more than 400 km long Bogda Shan lies in the eastern segment of the Chinese Tianshan, further extending eastwards into the Balikun–Harlik Mountains (Figure 1). These ranges jointly separate the Junggar and Turpan–Hami Basins. The Bogda basement is mainly composed of Carboniferous to Permian volcanic arc rocks associated with volcanioclastic sub-marine deposits (XBGMR 1993; Ma et al. 1997; Gu et al. 2000). These late Palaeozoic rocks have been significantly uplifted with present-day elevations of ~3–4 km above sea level (m.a.s.l.). In the topography of this mountain range, remarkable low-relief erosional surfaces that cross-cut basement rocks are exposed, but they are partly reworked by glacial erosion or river incision (e.g. Morin et al. 2019). The timing of exhumation of the Bogda Shan and the associated implications for the relationship (i.e. former connection) between the Junggar and Turpan–Hami Basins throughout the late Palaeozoic and Mesozoic remain highly debated (Carroll et al. 1995; Wartes et al. 2002; Greene et al. 2005; Tang et al. 2014; Ji et al. 2018; Wang et al. 2018a). Since late Palaeozoic-early Mesozoic thermochronological signals embedded in the basement rocks have been largely eroded by later tectonic events, current interpretations of the exhumation history of Bogda Shan rely heavily on sedimentological evidence (e.g. Fang et al. 2019; Wang et al. 2022 for recent comprehensive reviews).

Low-temperature thermochronology studies provide no consensus on the main exhumation phases of the Bogda basement. Some previous works within the Bogda Shan reveal pervasive young apparent (Oligocene–Miocene) apatite fission track ages (e.g. Shen et al. 2005; Wang et al. 2007, 2008a), which has led to the suggestion of significant late Cenozoic exhumation (Jiao et al. 2021). However, from a late Palaeozoic series in the western Bogda Shan (southern Urumqi; Figure 2), dominant Cretaceous cooling ages were obtained (Tang et al. 2015). Similarly, in the eastern Bogda and contiguous Balikun–Harlik Mountains, several recent studies argued for late Mesozoic exhumation and mountain building rather than Cenozoic (e.g. Gillespie et al. 2017a; Chen et al. 2020a; He et al. 2022a). The preservation of numerous planation surfaces along the Bogda–Harlik mountain chain (Figure 1; Cunningham et al. 2003; Morin et al. 2019) does not support intense regional denudation as compared to the present-day Chinese South Tianshan (e.g. Chang et al. 2021), and rather favours limited Cenozoic exhumation and denudation.

The very young cooling ages from the Bogda Shan were obtained some time ago and were fundamentally questioned by recent studies. However, these studies focused more on the Balikun–Harlik Mountains to the

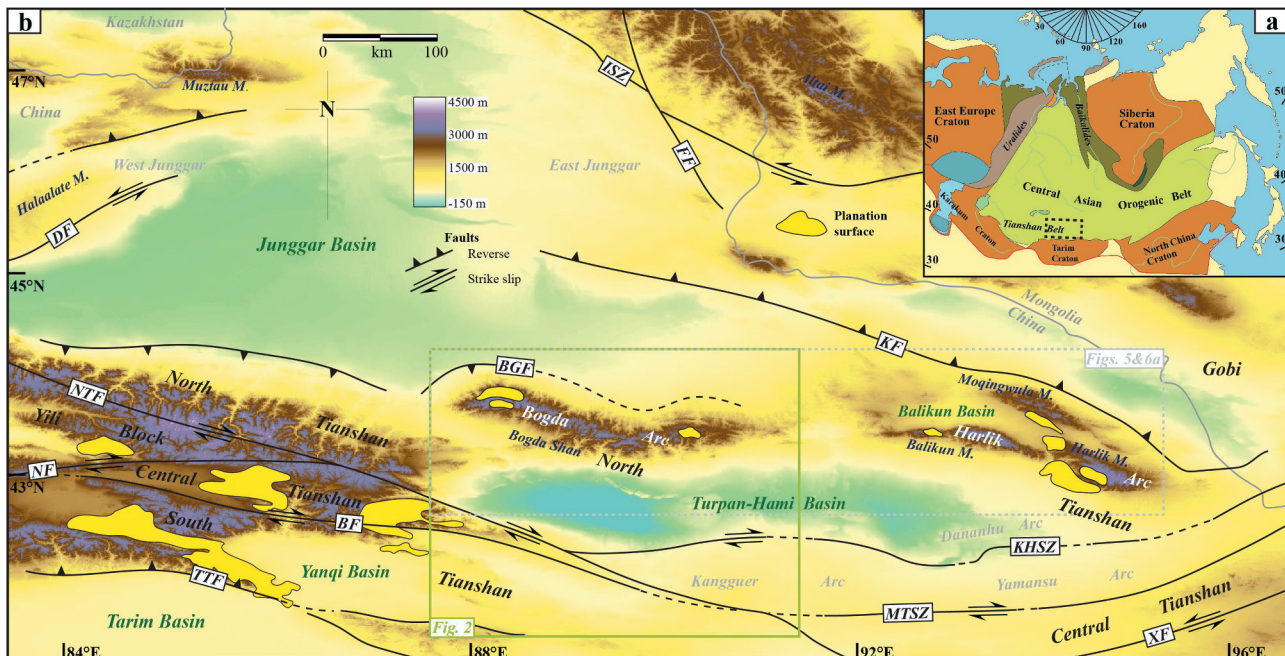


Figure 1. (a) Simplified sketch of the Central Asian orogenic belt (modified after Şengör et al. 1993) showing the location of the Bogda study area. (b) Simplified topographic map of the eastern Chinese Tianshan and adjacent areas, showing main tectonic units and major faults. Abbreviations: M. = mountains; BF = Baluntai fault; BGF = Bogda fault; DF = Dalabute fault; FF = Fuyun fault; ISZ = Irtyshev shear zone; KF = Kalamaili fault; KHSZ = Kangguer-Huangshan shear zone; MTSZ = Main Tianshan shear zone; NF = Nalati fault; NTF = North Tianshan fault; TTF = Tarim thrust fault.

east without a direct re-evaluation of the unconvincing thermochronological data of the Bogda Shan. It thus seems timely to reassess the Meso-Cenozoic thermo-tectonic history of the wider Bogda Shan area, and, subsequently, re-evaluate the impact of the Cenozoic India-Asia collision and continued convergence on this mountain range. In this work, we present new apatite fission track thermochronology for pre-Cenozoic crystalline rocks (e.g. Carboniferous meta-sandstones and Palaeozoic and Mesozoic felsic dikes) collected from the northern slopes of the Bogda Shan (southwest of the Mulei; Figure 2) and from its westernmost area (southern Urumqi). All of them are very close to the sampling locations in previous studies (e.g. Wang *et al.* 2007, 2008a). We also analysed three sedimentary samples (Jurassic to Palaeogene) from the neighbouring

basins as detrital AFT data may provide additional constraints on the extent of Meso-Cenozoic denudation. Combined with the published thermochronological and structural data, a clearer picture for the thermo-tectonic history of the ca. 700 km long Bogda-Harlik mountain chain, and a revised temporal framework for the intra-continental reactivation of the Chinese North Tianshan are presented.

2. Geological background

The ~E-W striking Tianshan belt is a major tectonic mosaic in the southwestern part of the Central Asian Orogenic Belt (CAOB) (e.g. Allen *et al.* 1992; Gao *et al.* 1998; Charvet *et al.* 2007; Xiao *et al.* 2013). The CAOB extends from the Uralides to the Pacific and is the

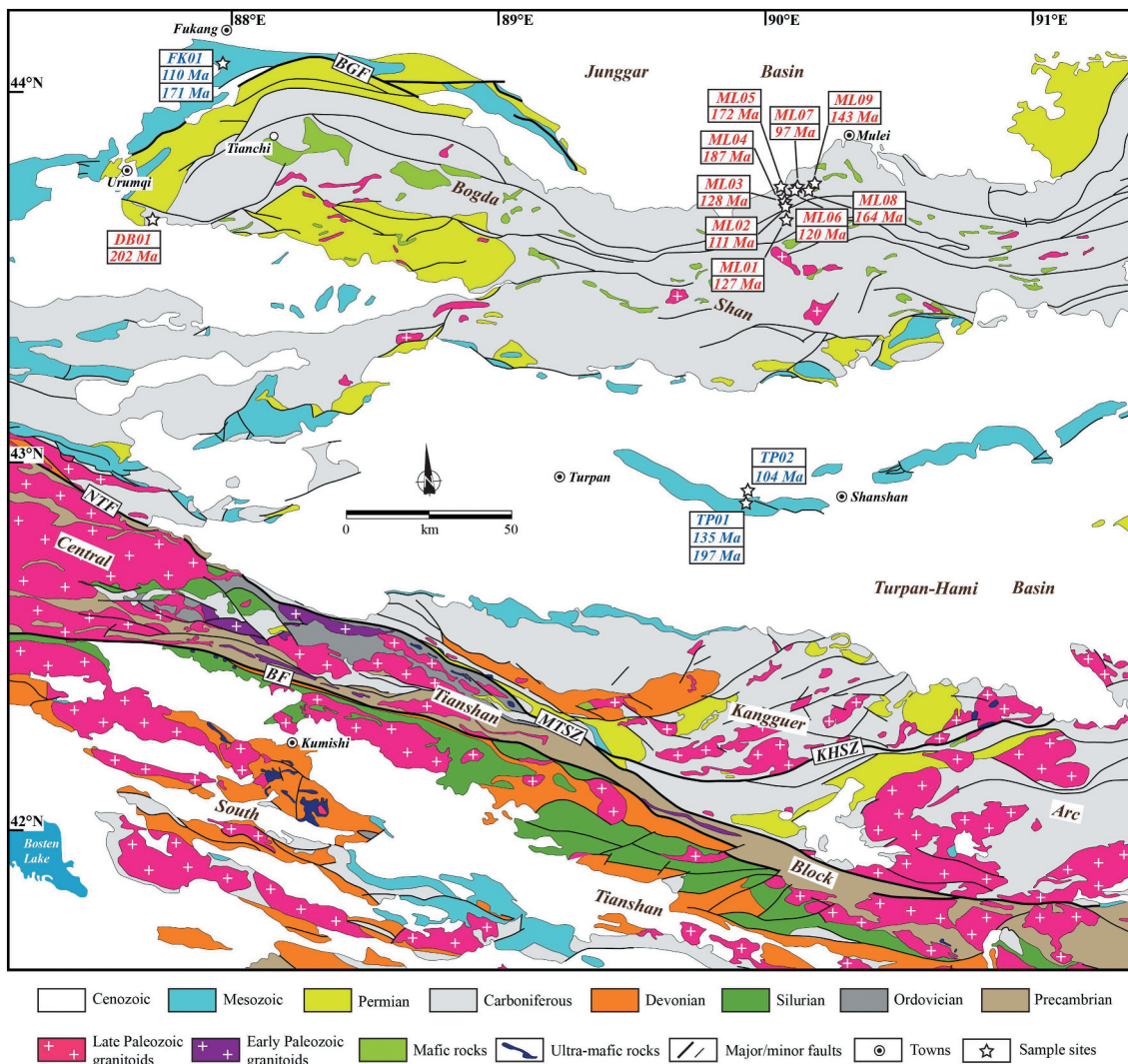


Figure 2. Simplified geological map of the Bogda Shan and adjoining regions (modified from XIGMR 2007). The location of our sample sites, with indication of apatite fission track ages (red for Palaeozoic basement rocks and blue for peak ages of the detrital samples). Abbreviations: BF = Baluntai fault; BGF = Bogda fault; KHSZ = Kangguer-Huangshan shear zone; MTSZ = Main Tianshan shear zone; NTF = North Tianshan fault.

world's largest preserved accretionary orogen ([Figure 1a](#)). It formed during the Neoproterozoic–Palaeozoic, including the subduction of the Palaeo-Asian oceanic slab, and successive amalgamation and multiple collisions of numerous micro-continents, island arcs, and accretionary wedges ([Mossakovskiy et al. 1993; Windley et al. 2007; Xiao et al. 2008; Wilhem et al. 2012; Kröner et al. 2014](#)). In the Mesozoic and Cenozoic, the ancestral Tianshan belt underwent protracted reactivation and was subjected to intense intra-continental compression and uplift, as a response to accretions and collisions at the southern Eurasian margins ([Molnar and Tapponnier 1975; Dumitru et al. 2001; De Grave et al. 2007; Glorie et al. 2010, 2011, 2012; Glorie and De Grave 2016; Yin et al. 2018; He et al. 2022a](#)).

2.1. Tectonic division of the Chinese Tianshan belt

The Chinese segment of the Tianshan belt is located between the Tarim Basin to the south and the Junggar Basin to the north ([Figure 1](#)). It is geologically divided into four units, i.e. the South Tianshan, Yili Block, Central Tianshan, and North Tianshan, based on different basement natures and tectonic settings (e.g. [Charvet et al. 2007; Wang et al. 2008b; Gao et al. 2011](#)). These units are separated by major suture zones and/or strike-slip shear zones ([Figure 1; Charvet et al. 2011; Wang et al. 2011; He et al. 2021a](#)).

The South Tianshan is bounded by the Nalati–Baluntai faults in the north and the Tarim thrust fault in the south ([Figure 1](#)). This domain is mainly composed of Ordovician-Carboniferous carbonate and marine clastic sediments, and Permian volcanic rocks ([Gao et al. 1998; Xiao et al. 2013; Alexeev et al. 2015](#)). A remarkable feature of the South Tianshan is the occurrence of Silurian–Devonian ophiolitic mélange along its southern margin, which have been interpreted as nappes derived from the north ([Han et al. 2011; Xiao et al. 2013](#) or remnants of back-arc basins ([Wang et al. 2018b; Zhong et al. 2019](#)). The Yili Block and Central Tianshan are two major continental blocks underlain by Precambrian crystalline basement rocks that were intruded by various Palaeozoic granitic plutons ([Wang et al. 2014a; Zhong et al. 2015; He et al. 2018; Zhu et al. 2019](#)). These two micro-continents were assembled due to the consumption of the intervening Terskey Ocean in the early Palaeozoic ([Qian et al. 2009; Han et al. 2015](#).

The North Tianshan is an accretionary complex separated from the Yili Block and Central Tianshan by the North Tianshan fault and the Main Tianshan shear zone ([Figure 1](#)). This domain includes a series of island arcs (i.e. the Bogda, Harlik, Dananhu, and Yamansu Arcs) that mainly consist of late Palaeozoic sedimentary-volcanic

strata and granitic rocks ([Xiao et al. 2009; Zhang et al. 2016; Ni et al. 2021](#)). It is generally considered that the North Tianshan was formed by the southward subduction of the Junggar Ocean – which had opened in the early Palaeozoic and existed until the early Carboniferous – and associated accretion events ([Ma et al. 1997; Xiao et al. 2004; Zhu et al. 2009; Han et al. 2010](#)). In the Permian, the southern part of the North Tianshan was subjected to large-scale post-collisional dextral transcurrent tectonics ([Wang et al. 2008c](#), with the emplacement of syn-kinematic plutons ([Wang et al. 2014b](#)).

2.2. The Bogda Shan

The Bogda Shan is a ridge underlain by rocks of the Bogda Arc. It is an anticlinal structure located in the central Chinese North Tianshan ([Figure 1](#)), and mainly comprises Carboniferous-Permian marine volcanic, pyroclastic, and carbonate rocks ([Figure 2; XBGMR \(Xinjiang Bureau of Geology and Mineral Resources\) 1993; Gu et al. 2000](#)). In this study, all of our Bogda samples are from Carboniferous strata and associated coeval felsic dikes. The Carboniferous strata are ~1200–1800 m thick and can be divided into three formations ([XBGMR \(Xinjiang Bureau of Geology and Mineral Resources\) 1993](#)). The lower Carboniferous Qijiaojing Formation is composed of marine tuffaceous sandstone, and volcanic ignimbrite and lava ([Gu et al. 2000; Xie et al. 2016a](#)). The upper Carboniferous Liushugou and Qijiagou Formations mainly contain shallow marine sandstone, mudstone, and limestone ([Carroll et al. 1995](#), associated with submarine basalt, basaltic anesite and rhyolite ([Shu et al. 2005; Gao et al. 2014](#)). The magmatic activity of the Bogda Arc mainly occurred during the Carboniferous to Permian (~347 Ma to ~265 Ma; [Chen et al. 2011, 2013; Shu et al. 2011; Xie et al. 2016b](#)).

The Bogda Shan has bilateral vergence with neighbouring basins that are tapered fold-and-thrust belts in active development stages, forming a positive flower structure that controls regional exhumation (e.g. [Cunningham et al. 2003; Cunningham 2021](#)). Although there is no agreement on major episodes of uplift and exhumation of the Bogda Shan, intense relief generation occurred in the Meso-Cenozoic, with late Palaeozoic (meta-) sedimentary basement over-thrusting the foreland strata ([Figures 1 and 2](#). Based on a summary of sedimentary data in the North Tianshan and southern Junggar, [Fang et al. \(2019\)](#) recently proposed that the initial uplift of the Bogda Shan may have occurred in the Early Jurassic. In the eastward continuation of the Bogda Shan, i.e. the Balikun–Harlik Mountains, widespread Cretaceous basement cooling is well documented by



several recent low-temperature thermochronological studies (e.g. Gillespie *et al.* 2017a; Chen *et al.* 2020a; He *et al.* 2022a).

2.3. The Turpan-Hami Basin

The Turpan-Hami (Tu-Ha) Basin is an intermontane basin within the North Tianshan and contains continental Meso-Cenozoic sedimentary sequences (Figures 1b and 2; XBGMR 1978). The basement of the Tu-Ha Basin is considered to be Ordovician to Carboniferous with accretionary (meta-) sedimentary rocks and oceanic crustal fragments (Allen *et al.* 1995; Carroll *et al.* 1995). It became a continental basin in the Permian and has evolved into a foreland basin since the Jurassic (Allen *et al.* 1992; Hendrix *et al.* 1992, 1995). Provenance analyses suggest that the Bogda–Harlik Arcs and the Central Tianshan have been the main sediment source areas for this basin since the Middle-Late Jurassic due to their tectonic uplift (e.g. Greene *et al.* 2005; Fang *et al.* 2019; Shen *et al.* 2020). In the western part of the basin, the Mesozoic strata reach over ~3 km in total thickness, while the sediment thickness of the Cenozoic cover is generally less than ~1.5 km (XBGMR (Xinjiang Bureau of Geology and Mineral Resources) 1978). Structurally, the Jurassic sequences are juxtaposed against Cenozoic strata here, and outspoken late Oligocene-early Miocene compressional deformation has been documented as well (XBGMR (Xinjiang Bureau of Geology and Mineral Resources) 1978; Zhu *et al.* 2006).

3. Samples and methodology

3.1. Sample information

In this work, we present new apatite fission track (AFT) data acquired from 10 Palaeozoic volcanic and granitoid rocks from the Bogda Shan, one Middle Jurassic sandstone from the southern margin of the Junggar Basin, and one Lower Cretaceous siltstone and one Palaeogene conglomerate from the Tu-Ha Basin (Figure 2). Sample descriptions including their locations are detailed in Supplementary Tables S1 and S2.

Most of the Palaeozoic rocks (ML01-09) were collected from the northern slope of the Bogda Shan (near the Mulei county; Figure 2) including a ~N-S traverse (ML01-05) with elevations ranging from 1396 m to 1696 m (Table S1). Samples ML02 and ML06 were taken from felsic dikes that intruded the late Carboniferous volcanic sequences (Liushugou Formation), ML02 is a narrow Jurassic (~174 Ma) intrusion, and ML06 has a latest Carboniferous crystallization age of ~304 Ma (Table S1). In the western Bogda Shan,

the volcaniclastic rock DB01 is from the upper Carboniferous strata (Qijiagou Formation) with a depositional age of ~311–297 Ma (Shu *et al.* 2011; Xie *et al.* 2016a).

3.2. Apatite fission track dating method

The AFT analyses (external detector method) were carried out at the Laboratory for Mineralogy and Petrology, Ghent University (e.g. De Grave *et al.* 2012; Nachtergael *et al.* 2018; He *et al.* 2021b). Spontaneous tracks in apatite were etched in 5.5 M HNO₃ solution for 20 s at 21°C. Apatite mounts were covered with a U-free external muscovite detector (Goodfellow® clear ruby) and irradiated with thermal neutrons to produce induced ²³⁵U fission tracks. We used the IRMM-540 dosimeter glasses (De Corte *et al.* 1998) to monitor the thermal neutron fluence. Irradiation was performed at the Belgian Reactor 1 facility of the Belgian Nuclear Research Centre (De Grave *et al.* 2010). Induced tracks were etched in the muscovite external detector with 40% HF for 40 min at 20°C.

Track densities were counted on a fully motorized Nikon Eclipse Ni-E microscope, equipped with a Nikon DS-Ri2 camera. The microscope and camera are linked to a computer with Nikon NIS Elements Advanced Research software, complemented with an in-house macro-enabled Microsoft Excel sheet (TrackFlow β) (Van Ranst *et al.* 2020). The obtained AFT ages are reported as conventional ζ -ages (Hurford 1990) with an overall weighted mean zeta of $310.0 \pm 2.7 \text{ a.cm}^2$ (Analyst Z. He), based on multiple Durango and Fish Canyon Tuff apatite standards (Hurford and Hammerschmidt 1985; McDowell *et al.* 2005). Central ages (Vermeesch 2009) for each sample are given as well. For samples that yielded enough apatite grains, a second set of mounts was made and subjected to ²⁵²Cf irradiation (Donelick and Miller 1991) at The University of Adelaide to enhance the number of measurable confined fission tracks. Confined track lengths and their angles to the crystallographic c-axis were measured using a 100x plan apochromat class objective and a 2x secondary optical magnification (Nikon DSC zooming port).

3.3. Thermal history modelling

To constrain the cooling and exhumation histories of the collected rocks, inverse thermal history modelling was performed following a multi-step approach in the QTQt package (Gallagher 2012). This program applies the Markov-Chain Monte-Carlo search algorithm (Gallagher *et al.* 2009) to predict a thermal history based on the AFT age and length data. We used the annealing model of

Ketcham *et al.* (2007), with D_{par} as the kinetic parameter. Thermal history modelling was conducted on four samples that yielded sufficient numbers (all >100) of confined tracks (Supplementary Table S3). The modelling time range was set as central age \pm central age (Ma) and $70 \pm 70^\circ\text{C}$ for the temperature. The present surface temperature was set as $15 \pm 10^\circ\text{C}$, which is a realistic value for the current conditions in the Bogda Shan. In order to avoid over-interpretation and bias of the modelling results, the QTQt models were performed without any external time-temperature constraints. We first ran the algorithm for 10,000 burn-in and 50,000 post-burn iterations in order to find the appropriate search parameters. Subsequently, we ran 200,000 iterations with a burn-in of 100,000 for independent sample inversion.

4. Results

4.1. Basement apatite fission track results

The AFT results of the 10 basement samples are listed in Table S3 and displayed in Figure 2. Although a few samples only yield less than 10 suitable grains due to the low apatite yield in the fine-grained tuffaceous sandstones, all of them passed the χ^2 test of homogeneity for the AFT age. When $P(\chi^2) > 5\%$, the inter-sample variation is considered to adhere to a natural Poissonian distribution (Galbraith and Green 1990). Apatite grains from igneous or metamorphic rock have witnessed the same time-temperature path since initial cooling and are therefore expected to belong to a single age population, thus passing the χ^2 test. Radial plots produced by IsoplotR (Vermeesch 2018) for each sample are presented in Supplementary Figure S1. The obtained apparent AFT ages are predominantly Mesozoic, ranging from the latest Triassic to the Late Cretaceous. From the southern Mulei area, nine samples originating from elevations between ~ 1746 – 1369 m yield Jurassic–Cretaceous ages ranging from 189 ± 17 Ma to 91 ± 36 Ma. Sample DB01 that was taken from the southern Urumqi area and displays a Late Triassic age of 207 ± 12 Ma (Supplementary Table S3).

The majority of the samples did not yield adequate numbers of measurable confined tracks due to the limited apatite grains extracted or their poor quality (small grain size). After ^{252}Cf irradiation on duplicate mounts, we obtained >70 confined track length measurements (two of them >100) on samples ML05, ML08, and DB01, passing the proposed minimum requirements for producing a representative histogram (e.g. Barbarand *et al.* 2003). Since for sample ML09 only 12 lengths could be measured, these results will not be used for further discussion. When plotting track lengths *versus* angle to

the c-axis (for samples ML05, ML08, and DB01; Supplementary Figure S2), all samples show a relatively high degree of track length isotropy (i.e. confined track lengths do not tend to become shorter when their angles to the c-axis increase). This means that they do not meet the presumptions to perform c-axis projection ‘correction’ (Ketcham *et al.* 2007), we thus decided that c-axis projection is not appropriate for this dataset.

4.2. Detrital apatite fission track results

Regarding the detrital samples, 100 grains were analysed for each sample, and AFT results are presented in Supplementary Table S2. The Middle Jurassic sandstone FK01 (northern Bogda Shan) shows individual AFT ages ranging between ~ 437 and ~ 62 Ma ($P(\chi^2) < 5\%$), which can be statistically decomposed into two age populations: a Middle Jurassic age of ~ 171 Ma and an Early Cretaceous age of ~ 110 Ma (Figure 3a). Considering the occurrence of both older and younger single grain AFT ages with respect to its stratigraphic age, the AFT system of the Middle Jurassic sample FK01 should have experienced a certain degree of partial (but not complete) resetting. Higher up in the stratigraphic sequence, the Lower Cretaceous siltstone sample (Tu-Ha Basin) TP01 also failed the χ^2 test with high dispersion, and single grain age results can be separated into two populations of ~ 197 (Early Jurassic) and ~ 135 Ma (Early Cretaceous) (Figure 3b). It contains a large number of single grain AFT ages that are comparable or older in age with regard to the stratigraphic age, indicating that the Lower Cretaceous strata in the study area only experienced very slight thermal resetting. Consequently, the AFT data preserves provenance information. Palaeogene sample TP02 (Tu-Ha Basin) only shows one age population with a central age of ~ 104 Ma, and almost all the single grain detrital AFT ages obtained for this rock are Mesozoic (Figure 3c), suggesting that apatite grains in this conglomerate sample entirely retained the fission tracks that were previously accumulated in the source areas.

4.3. Thermal history modelling results

In our dataset, all three acquired models give the expected t-T paths showing relatively slow to moderate cooling ($<1^\circ\text{C/Ma}$) since the Triassic (Figure 4). Sample ML05 displays a quasi linear, prolonged cooling throughout the Meso-Cenozoic, with a long residence (>100 Ma) within the apatite partial annealing zone (APAZ; ~ 120 – 60°C). Based on AFT age and sufficient length data ($n = 100$), the thermal history model for sample ML08 is well constrained and indicates a clear two-stage

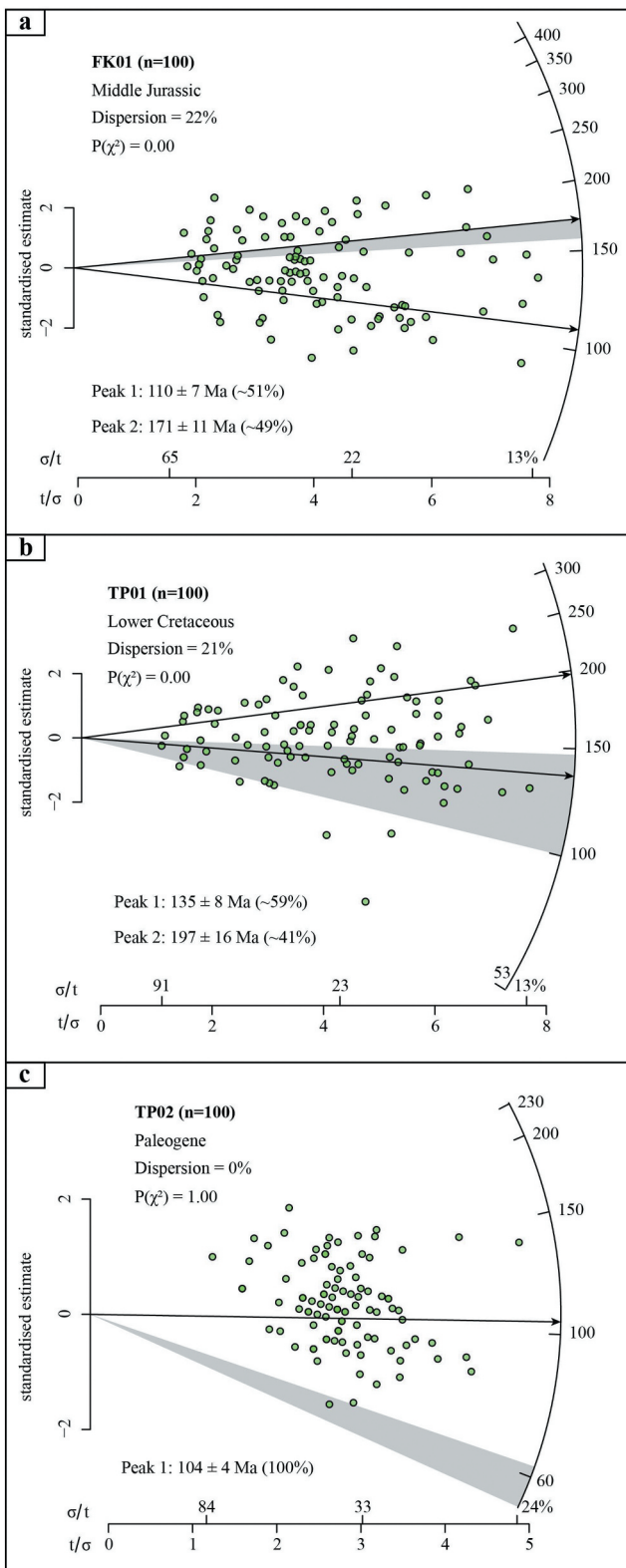


Figure 3. Radial plots of AFT single-grain ages for the Mesozoic detrital samples. Radial plots, dispersion and the $P(\chi^2)$ test and peak ages were obtained through IsoplotR (Vermeech 2018). The depositional ages of the strata are indicated by the shaded area.

cooling, i.e. a slow to slightly moderate rock cooling is modelled to have lasted until the Early Cretaceous, followed by a long-term cooling stagnation to the present. Moderate cooling, i.e. more rapid as compared to ML06, is observed for the western Bogda sample DB01 between ~250 and ~180 Ma (Figure 4). This cooling phase brought the rock to near-surface conditions. The late Cenozoic cooling perceived in the models appears outside of the thermal sensitivity window of the AFT system (i.e. outside the APAZ) and is regarded as a common software artefact (e.g. Ketcham *et al.* 1999) and will hence not be discussed.

5. Interpretations and discussion

5.1. Thermochronological data

The majority of the dated basement rocks, including slightly metamorphosed Carboniferous tuffaceous sandstones and felsic dikes, come from outcrops in southern Mulei county (Figure 2). The obtained results dominantly render Jurassic to Cretaceous apparent AFT ages (both zeta and central ages). Hence, in the northern flank of the Bogda Shan, a clear Mesozoic low-temperature thermochronometric signal is preserved. Nevertheless, these ages display a certain degree of dispersion and variability, notwithstanding that the nine dated basement rocks (ML01-09) were collected in relative proximity of one another, along vertical profiles with only minor differences in elevation (<~400 m; Table S1). We suggest that they may have stayed in the APAZ for relatively long time before their final exhumation. This is indeed corroborated by the two representative inverse thermal history models (Figure 4), resulting in significant partial annealing of the fission tracks and age variability within the exhumed APAZ (e.g. Malusà and Fitzgerald 2019). Inverse thermal history modelling results of samples ML05 and ML08 suggest slow to slightly moderate cooling throughout the Mesozoic. ML05 cooled from ~100 to ~60°C over a span of >100 Ma, ML08 shows a residence of ~40 Ma (Early-Middle Jurassic) in the APAZ with an average cooling rate of ~0.7–0.8°C/Ma (Figure 4). Furthermore, the thermal history model for ML08 indicates a significantly slower cooling rate since the earliest Cretaceous. This suggests that the northern Bogda Shan only experienced relatively slow exhumation without significant basemant cooling since the early Mesozoic. The two-stage cooling history of ML08 shows a more rapid basement cooling rate in the Jurassic (Figure 4). We propose that the distal effects of the collision of the peri-Gondwanan Qiangtang block to the Eurasian

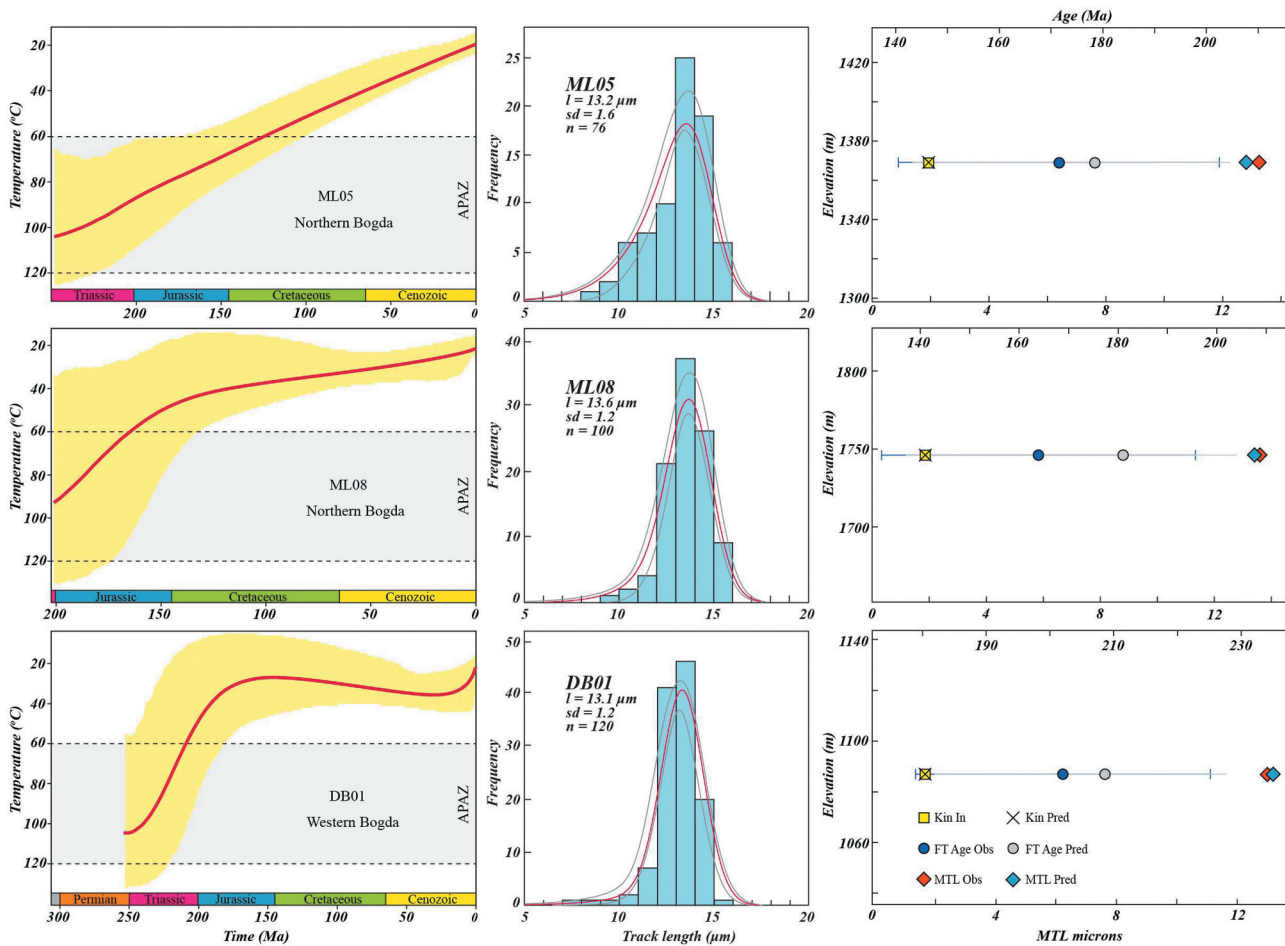


Figure 4. Thermal history models (left panel) for samples ML-05 (upper), ML08 (middle), and DB01 (lower), reconstructed by the QTQt modelling software (Gallagher 2012). The red line is the expected model, the yellow envelope reflects 95% confidence interval. The input parameters from the confined track length measurements and fit of the most likely model are given in the middle panel. The predicted and observed values for the kinetic parameter (D_{par}), apatite fission track age and mean track length are shown in the right panel. See text for discussion.

continent along its southern margin (e.g. De Grave *et al.* 2007; Glorie *et al.* 2010; Jolivet *et al.* 2013; He *et al.* 2022b), to some extent, was the driving force for this.

In the western Bogda, the obtained results for the Carboniferous tuff DB01 also demonstrate an early Mesozoic slightly moderate ($\sim 1.0\text{--}0.9^\circ\text{C/Ma}$) cooling phase (Figure 4). Compared with the (expected) cooling paths obtained for the northern Bogda flank, the moderate cooling there initiated earlier in the Early Triassic and lasted until the Jurassic. Based on a summarization of literature, it is suggested that at the end of the Carboniferous ($\sim 310\text{--}300$ Ma), the eastern Chinese Tianshan (including the entire Bogda-Harlik Arcs) and the Beishan belt were eventually welded as a result of the synchronous closure of the (eastern) North Tianshan and South Tianshan Oceans (Han and Zhao 2018; and references therein). Therefore, the Triassic-Jurassic cooling in the western Bogda was not likely related to the closure of the ancient Tianshan oceans, but occurred in

an intra-continental setting. We hence favour the interpretation that the far-field stresses related to the coeval convergence between Eurasia and the Qiangtang block contributed to the intra-plate exhumation along the Bogda Shan. With regard to the whole Tianshan belt, Triassic-Jurassic basement cooling signals are not widely preserved (by low-temperature thermochronology) compared to the widely recognized Cretaceous signals. In the Kyrgyz-Kazakh and the western Chinese Tianshan, small pockets of Late Triassic-Middle Jurassic AFT ages have been identified in uplifted plateaus such as the Song-Kul and Issyk-Kul lakes (De Grave *et al.* 2011, 2013; Macaulay *et al.* 2014), in low-relief sections of the Tianshan such as the Tarbagatai, West Junggar, and Junggar Alatau mountains (Glorie *et al.* 2019; Gillespie *et al.* 2020, 2021), and along large-scale strike-slip faults such as the Talas-Fergana and Nalati faults (Jepson *et al.* 2021; He *et al.* 2022b). The inverse thermal history modelling results in this study reveal that early Mesozoic



basement cooling also occurred in the eastern Chinese Tianshan, albeit with marked slower cooling rates. In case of the Bogda Shan, the lack of major (pre-Mesozoic) inherited fault reactivations (e.g. the NTF-MTSZ, BF, and KHSZ; [Figures 1b and 2](#)) possibly accounts for the less intensive deformation and slower exhumation rates.

As to the detrital results from the northern Bogda (southern Junggar Basin), the Middle Jurassic sandstone FK01 is characterized by broadly distributed Triassic-Cretaceous single grain AFT ages. The occurrence of the young mid-Cretaceous age peak (~110 Ma) indicates post-depositional burial resetting in this sample site. According to available field mapping results ([XBGMR 1965](#)), the overlying Upper Jurassic to Cretaceous strata reach a thickness of ~3.7–5.1 km in the southern Junggar, creating sufficient sedimentary burial that should have been capable of at least partly resetting the AFT system. In addition, we evaluated the relation between AFT age and ^{238}U concentration on this sample ([Supplementary Figure S3](#)). It is observed that the younger (Peak 1) ages generally correlate with higher ^{238}U concentrations, indicating that this set of apatite grains may have experienced more extensive AFT annealing than Peak 2 grains due to a chemical control (e.g. [Hendriks and Redfield 2005](#); [Fernie et al. 2018](#)). Therefore, the ~171 Ma age population (generally coeval with the depositional age; [Figure 3a](#)) represents the inherited AFT age signals from the source areas, whereas the ~110 Ma age peak probably reflects a post-resetting event in the mid-Cretaceous. Based on a summary of published detrital zircon U-Pb data and sedimentary analyses, it is suggested that the North Tianshan was the main source terrane for the sediments in the southern Junggar Basin during the Jurassic (e.g. [Fang et al. 2019](#); [Wang et al. 2022](#)). Hence, the Late Triassic-Middle Jurassic AFT cooling ages were not only recorded by the basement rocks in the Bogda Shan ([Supplementary Table S3](#)), the neighbouring basins also received coeval thermochronological signals. Early to mid-Cretaceous enhanced basement cooling and fault reactivation have been widely recognized in the eastern Chinese Tianshan, generally under a compressional regime ([He et al. 2022a](#); and references therein). The mid-Cretaceous age peak observed in FK01 is much younger than its depositional age, and thus may represent a tectonic reactivation that resulted in deformation and exhumation of the Jurassic strata.

In the central Tu-Ha Basin, the Lower Cretaceous and Palaeogene detrital samples TP01 and TP02 experienced almost no post-depositional reheating and largely preserved their inherited AFT signals from the source regions ([Figure 3b-c](#)). According to published detrital

zircon geochronological data and associated provenance analyses (e.g. [Fang et al. 2019](#); [Shen et al. 2020](#)), detritus in the Tu-Ha Basin dominantly originated from the North Tianshan (including the Bogda-Harlik and the Kangguer Arcs; [Figure 2](#)) during the Late Jurassic to late Palaeogene. The broad range of Jurassic to Cretaceous AFT cooling ages in these two samples gives three populations of ~197, ~135, and ~104 Ma, respectively. Together with the results presented by the southern Junggar sample FK01, they provide evidence for uplift and erosion in the neighbouring North Tianshan during the Jurassic to mid-Cretaceous. The Mesozoic thermo-tectonic history of the Tianshan belt and adjacent areas was dominated by deformation induced by the collision of Cimmerian continental fragments (e.g. the Qiangtang and Lhasa blocks) with the southern Eurasian margin (e.g. [De Grave et al. 2012](#); [Käßner et al. 2017](#); [Jepson et al. 2018a](#)), which generated sustained contraction in a post-collisional setting. As a result, the spread of Jurassic-Cretaceous AFT single grain ages in these three detrital samples is not unexpected. Furthermore, the distinguished age populations (peaks) are in good agreement with the basement cooling ages (both AFT and apatite (U-Th)/He) reported from the Harlik, Kangguer, and Yamansu Arcs in the eastern Chinese Tianshan (e.g. [Gillespie et al. 2017a](#); [Sun et al. 2021](#); [He et al. 2022a](#)). The denudation of these basement rocks hence has provided a large volume of sediments to the adjoining and long-lived basins.

5.2. Mesozoic building of the Bogda-Balkun-Harlik mountain chain

Our low-temperature thermochronological results show that the Bogda Shan experienced a thermo-tectonic history comparable to the other mountain ranges of the Tianshan both to the west (e.g. [Jolivet et al. 2010](#); [Glorie and De Grave 2016](#); [He et al. 2022b](#)) and to the east (e.g. [Gillespie et al. 2017a, 2017b](#); [Chen et al. 2020a](#); [He et al. 2022a](#)). Jurassic to Cretaceous AFT central ages are by far the most common, while some older (preserved) Triassic ages can occasionally be recognized. Generally, in the areas outside the modern fault-bounded ranges or away from major inherited structures in the Tianshan and adjacent areas, a large area of pre-Mesozoic (basement) rocks did not experience significant exhumation-induced basement cooling during the subsequent Mesozoic and Cenozoic tectonic deformation ([He 2022](#)). Bogda Shan does not host old Proterozoic-Palaeozoic sutures nor shear zones ([Figure 1b](#)). A major thrust fault (i.e. the Bogda fault) has developed along its northwestern margin ([Figure 2](#)), but it is documented as a late Cenozoic brittle

fault and its eastward extension is quite limited according to available geological maps (e.g. XIGMR (Xi'an Institute of Geology and Mineral Resources) 2007). As a result, the Bogda Shan seemed to have acted as a relatively rigid block experiencing only slow to moderate exhumation (like many other continental blocks in the CAOB) during the long-term intra-continental evolution, as revealed by our new thermal history information obtained on the dated Palaeozoic rocks (Figure 4).

Wang *et al.* (2008a) presented numerous Cenozoic AFT ages from the Bogda–Harlik mountain chain and suggested that major uplift of the eastern Chinese Tianshan took place during the Oligocene–Miocene (~30–20 Ma). This thermochronological dataset was then further used for a 2-D thermo-kinematic modelling approach to quantitatively constrain the growth of the mountain range in a recent paper (Jiao *et al.* 2021). However, Cenozoic intense uplifting of the Bogda–Balikun–Harlik mountains has been challenged by several recent works. In the western Bogda Shan, Tang *et al.* (2015) analysed several Carboniferous to Permian sandstones using the AFT method and identified moderate to slow cooling phases (<1.5–1.0°C/Ma within the APAZ) that initiated in the earliest Cretaceous, i.e. almost identical to our data presented here. In the southern Bogda, He *et al.* (2021b) dated two granitic rocks and obtained Jurassic central ages that were previously reported as being Late Cretaceous or even Miocene (~16–9 Ma; Wang *et al.* 2008a). Their thermal histories generally exhibit protracted slow cooling since the Triassic (Figure 4 in He *et al.* 2021b), which is highly comparable with the cooling paths of the northern Bogda flank samples ML05 and ML08 (Figure 4). Similarly, along the eastern part of the Bogda Shan, and the Balikun, Moqinwula (Dahei Shan), and Harlik Mountains in the easternmost Tianshan, a significant amount of low-temperature thermochronological (mainly AFT) data

acquired in recent studies (e.g. Gillespie *et al.* 2017a; Chen *et al.* 2020a, 2020b; He *et al.* 2022a) gave various Mesozoic cooling ages (Figure 5). Here, we demonstrate that samples taken in the southern Mulei and southeastern Urumqi areas, in very close vicinity to those from which apparent young Cenozoic AFT ages were previously reported (Figure 5), are in fact all Mesozoic in age. The related thermal history models generally reveal enhanced cooling phases during the Late Jurassic to Palaeogene, thus disproving the occurrence of unusual young Cenozoic ages and suggested late Cenozoic rapid exhumation.

Wang *et al.* (2007) presented a set of Cenozoic detrital AFT central ages (~59–12 Ma) for the Jurassic strata located in the southern Junggar Basin (northwestern Bogda), and these data were also incorporated into the inverse modelling performed by Jiao *et al.* (2021). These AFT central ages are significantly younger than their stratigraphic ages, implying that the whole sequence of Jurassic strata should have experienced complete thermal resetting with burial depths in excess of ~4–5 km. However, from the same outcrop, the Middle Jurassic sandstone FK01 in our study is found to have only experienced partial resetting containing a mixture of younger and older AFT single grain ages with respect to its depositional age (Figure 3a). Moreover, no Cenozoic single grain ages were recognized at all. As mentioned above, the Jurassic-Cretaceous strata in the southern Junggar Basin have a total maximum thickness of around 4.6 km. In large parts of the basin, this maximum thickness was not attained (XBGMR (Xinjiang Bureau of Geology and Mineral Resources) 1965). Therefore, only parts of the middle to lower sections of the Jurassic strata have been buried deep enough to experience temperatures exceeding ~120°C. It would be expected that a number of apatite grains preserved their inherited AFT information from the source, as is the

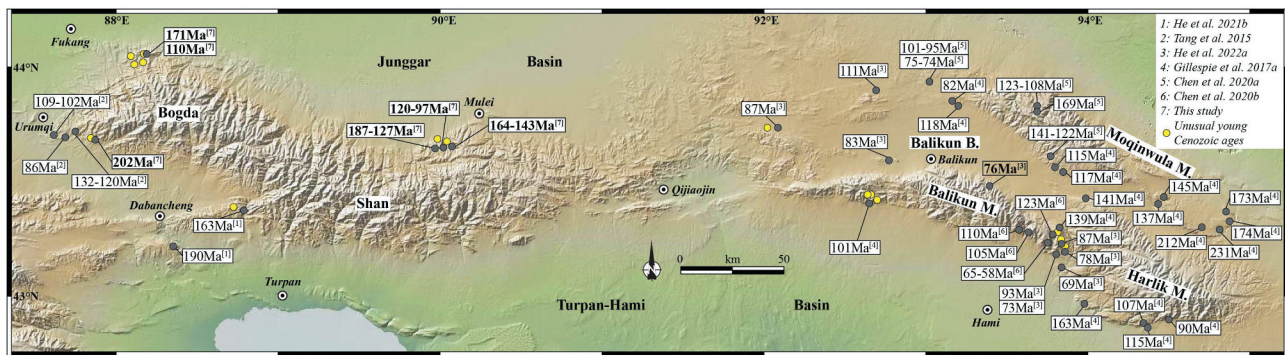


Figure 5. Simplified topographic map of the Bogda–Balikun –Harlik mountain chain (eastern Chinese Tianshan), showing published pre-Mesozoic basement AFT central ages (including data from this study). Sample locations of studied sites with anomalously young Cenozoic ages (Shen *et al.* 2005; Wang *et al.* 2007, 2008a) are also indicated. Data are from Tang *et al.* (2015); Gillespie *et al.* (2017a); Chen *et al.* (2020a), Chen *et al.* (2020b); He *et al.* (2021b), He *et al.* (2022a).



case for sample FK01 for example. On the other hand, the Chinese Tianshan belt and neighbouring basins experienced varying degrees of deformation during the Cretaceous generally under a contractional setting (e.g. Zhu *et al.* 2004, 2006; Yang *et al.* 2017; Wang *et al.* 2022; He *et al.* 2022a, 2022b). In the eastern and southern Junggar Basin, the Jurassic strata were deformed and folded as revealed by the seismic profile data (e.g. Yang *et al.* 2017; Wang *et al.* 2018c). Consequently, some deeper buried Jurassic sandstones might already have been exhumed into or even beyond the APAZ at certain periods in the Cretaceous, prior to the Cenozoic.

In addition, a lack of Cenozoic exhumation along the Bogda–Balikun–Harlik mountain chain is also supported by geomorphological observations. In the eastern Chinese Tianshan, a total of six major uplifted low-relief surfaces can be identified (Figure 6). Among them, an initial planation surface (P6; Figure 6g) that formed prior to the Late Cretaceous has been studied by low-

temperature thermochronology (Gillespie *et al.* 2017a). These authors suggested that this uplifted and tilted low-relief surface was reworked during the Late Cretaceous to Palaeocene (showing regional enhanced cooling) with no further posterior cooling. This implies that the southern Harlik Mountains experienced very limited exhumation during the Cenozoic. As to the low-relief surfaces in the Bogda Shan, our observations are in agreement with those formulated in Morin *et al.* (2019). The latter study makes a case for the existence of a Mesozoic planation surface at elevations of ~3500–4000 m in the western Bogda (P1; Figures 1b and 6b), which is around 1000–1500 m lower than the high Bogda range. This broad erosional surface crosscuts various Palaeozoic rocks and is reworked by recent glacier and river incision, making it look much less outspoken than the low-relief surfaces in the east (Figure 6). Therefore, the Bogda, Balikun, Moqinwula, and Harlik Mountains in the eastern Chinese Tianshan

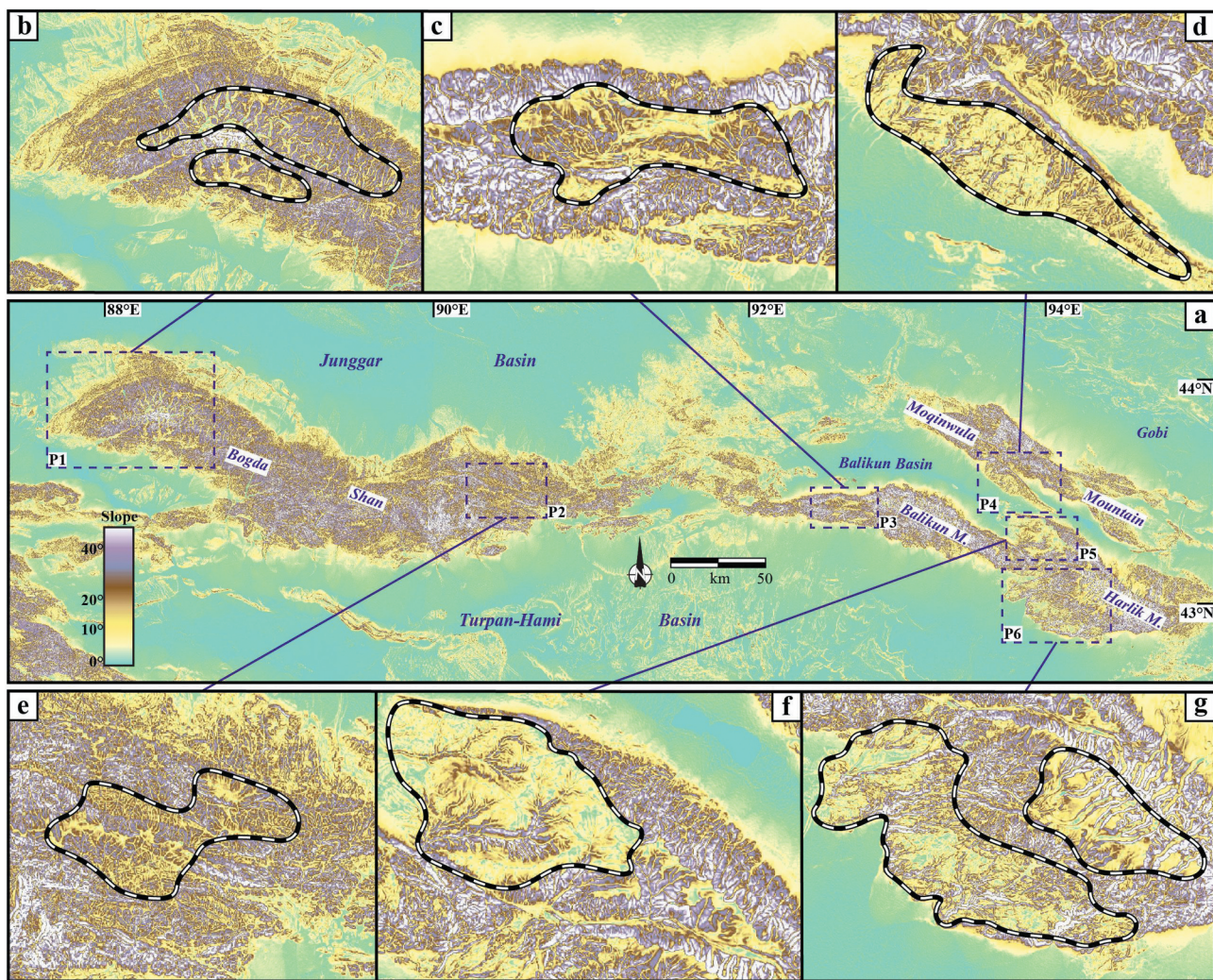


Figure 6. Slope map of the Bogda–Balikun–Harlik mountain chain (eastern Chinese Tianshan) showing distinct low-relief peneplanation surfaces.

display consistent topographic features, with the occurrence of widespread Mesozoic planation surfaces. This clearly seems to conflict with the notion that the Bogda Shan, and other ranges to the east, would have undergone significant late Cenozoic rapid exhumation ($>\sim 3$ –4 km within several million years).

In order to have a general view on the basement cooling and exhumation history of the Bogda–Balikun–Harlik mountain chain, we compiled the available thermal history models (based on basement low-temperature thermochronological data) from recent papers and this study (Figure 7a–c). The numerous acquired cooling paths generally reflect Mesozoic residence in the APAZ of the dated basement rocks from this long mountain chain, and almost all of them have cooled entirely through the APAZ before the Cenozoic. This indicates that there was substantially less than ~ 2 km exhumation during the Cenozoic, and could

account for the preservation of widespread Mesozoic planation surfaces in the mountain ranges. In addition, the compilation of the cooling curves also reveals that episodic enhanced basement cooling, which brought the rocks to the shallow crust, generally occurred in the Mesozoic (Figure 7). The widespread Jurassic and Cretaceous AFT ages recorded in the Meso-Cenozoic sedimentary rocks from the adjacent basins further provide detrital thermochronological evidence for substantial Mesozoic orogenic erosion, as revealed by the analysed detrital samples in this study.

Based on the discussion above, it is reasonable to come to the conclusion that the previously acquired young Cenozoic AFT ages along the Bogda–Balikun–Harlik mountain chain (e.g. Wang *et al.* 2008a), and the proposed Cenozoic ‘multi-stage uplift and growth’ of the Bogda Shan (e.g. Jiao *et al.* 2021) are disputable. Instead, the exhumation of shallow crustal rocks ($<\sim 2$ –4 km)

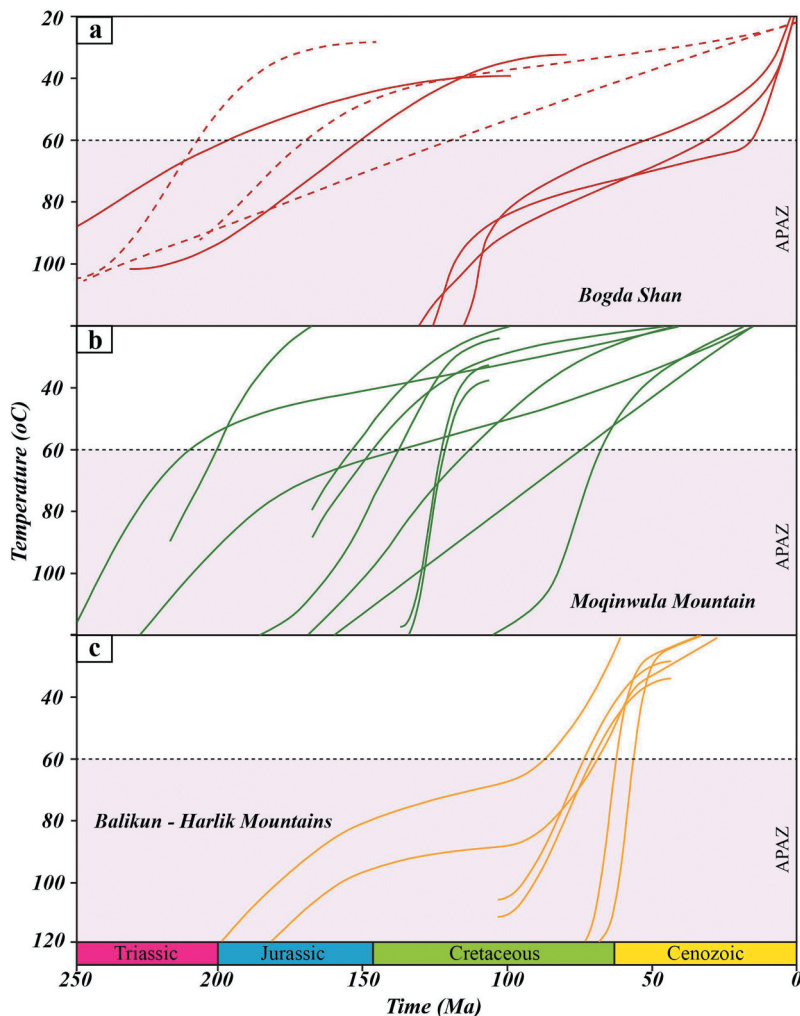


Figure 7. Modelled temperature-time paths (expected models) for basement samples from the Bogda, Moqinwula, and Balikun–Harlik Mountains (eastern Chinese Tianshan). Original data are from Tang *et al.* (2015); Gillespie *et al.* (2017a); Chen *et al.* (2020a), Chen *et al.* (2020b)); He *et al.* (2021b), He *et al.* (2022a)); and this study (highlighted by dashed lines). See text for detailed discussion.



through denudation in the eastern segment of the Chinese Tianshan seems to have mainly occurred in the Mesozoic.

5.3. Regional implications

Our findings in this study reveal that the Bogda Shan has not seen extensive Cenozoic exhumation akin to the present-day Pamirs or the southern Kyrgyz – Chinese Tianshan as previously considered. In contrast, Bogda Shan shows highly comparable topographic features (e.g. occurrence of elevated/uplifted low-relief surfaces) AFT ages, and a thermo-tectonic history (e.g. generally slow to moderate cooling since the early Mesozoic) similar to the Central Tianshan (Figure 1b; He *et al.* 2021b). A series of dismembered planation surfaces are distributed in the Yili block (western Chinese Tianshan) and the contiguous Tarbagatai Mountains–Junggar Alatau (eastern Kazakhstan Tianshan) (Morin *et al.* 2019). Large parts of these mountain ranges have generally experienced slow to moderate basement cooling since the Early Jurassic without detection of Cenozoic low-temperature thermochronological signals (e.g. Wang *et al.* 2018d, 2021; Glorie *et al.* 2019; Gillespie *et al.* 2021; Zhao *et al.* 2021; He *et al.* 2022b). Hence, it is suggested that the majority of the Chinese Tianshan belt and adjacent eastern Kazakh Tianshan experienced limited exhumation (<~1–2 km) during the Cenozoic, with consequential preservation of distinct Mesozoic low-relief surfaces.

This implies that, although the Cenozoic tectonic evolution of Central Asia was significantly influenced by the continued indentation of the Indian plate into the Eurasian continent (e.g. Molnar and Tapponnier 1975), the extent of far-field strain in Central Asia, associated with this tectonic event, is highly variable. In the southwestern Tianshan belt (central-southern Kyrgyz and southern Uzbek Tianshan), close to the western syntaxis of the Himalayas (the Pamirs), Eocene-Oligocene and Miocene deformation has been dated on the basis of AFT and apatite (U-Th)/He analyses (e.g. Glorie *et al.* 2011; De Grave *et al.* 2012; Macaulay *et al.* 2013, 2014; Bande *et al.* 2017; Jepson *et al.* 2018b). This is indicative of Cenozoic intense deformation and unroofing corresponding to tectonic reactivation induced by the India-Asia collision. The Chinese Tianshan, however, is geographically further north, and the stress generated from the south had to propagate through the large and stable Tarim Craton before reaching the Chinese Tianshan (Figure 1). In addition, a series of ~E-W-trending fold-and-thrusts belts occur along the southern Chinese Tianshan margin, which consist of >~10 km thick Mesozoic and Cenozoic clastic sediments

(Wang *et al.* 2001; Huang *et al.* 2006; Hubert-Ferrari *et al.* 2007). Structural and low-temperature thermochronological studies revealed that these intensively deformed belts have accommodated a significant amount of Cenozoic shortening between the Chinese Tianshan belt and the Tarim Craton (e.g. Chang *et al.* 2012, 2017, 2019). As a result, Cenozoic deformation of the (pre-Mesozoic) crystalline basement of the Chinese Tianshan was limited (e.g. Yin *et al.* 1998; Burchfiel *et al.* 1999), and old Mesozoic or even late Palaeozoic low-temperature thermochronological signals are largely preserved, especially in study areas away from major shear zones.

AFT data mainly yield information about cooling of the investigated rocks from ~120 to ~60°C, which corresponds to a depth of ~2–3 km in the crust. While cooling beneath ~60–50°C that corresponds to the last ~1.5–1 km of exhumation is not well constrained, this amount of exhumation is smaller but far from negligible. Along the eastern Chinese Tianshan (particularly the northern margin of the Bogda Shan), late Cenozoic reactivation is evident from structural relationships recognized in the field and topographic analyses (e.g. Wu *et al.* 2016, 2021, 2022; Wang *et al.* 2020). Therefore, Cenozoic (and ongoing) basement exhumation has affected the eastern Chinese Tianshan but has not resulted in deep denudation (>~1.5–1 km). Consequently, pre-Cenozoic AFT signals are predominantly preserved in the eastern Chinese Tianshan basement.

6. Conclusions

This study presents new basement and detrital apatite fission track (AFT) data from the Bogda Shan and the adjacent southern Junggar and central Turpan-Hami Basins. Based on a comprehensive re-evaluation of the Mesozoic to Cenozoic thermo-tectonic evolution of the Bogda Shan, we conclude that:

- (1) No Cenozoic basement AFT ages have been detected from the Bogda Shan. The sampled Palaeozoic rocks from the northern and western-most Bogda all display Mesozoic (mainly Jurassic to Cretaceous) apparent AFT ages, which are highly comparable with those from the Balikun, Moqinwula, and Harlik mountain ranges to the east.
- (2) The aforementioned conclusion clearly contradicts previously reported Cenozoic AFT ages and cooling histories for this mountain belt. This discrepancy could be explained by inappropriate laboratory procedures, such as etching protocols or calibration issues. However, most previous

- studies do not report laboratory conditions and thus this hypothesis cannot be satisfactorily tested.
- (3) The Jurassic sandstones in the southern Junggar Basin were not buried deeply enough to completely reset their AFT clock as previously considered. Apatites from the Middle Jurassic section were only partially reset, displaying both Middle Jurassic (~171 Ma) and mid-Cretaceous (~110 Ma) AFT cooling ages. The latter suggests sedimentary burial might have partially reset the AFT system, likely during the Cretaceous.
- (4) Lower Cretaceous and Palaeogene sedimentary rocks collected from the intermontane Turpan-Hami Basin show detrital AFT age populations of ~197, ~135, and ~104 Ma, which are coincident with the basement AFT cooling ages derived from the surrounding Chinese North Tianshan. There is no evidence for thermal resetting in any of the sampled sediments.
- (5) The Bogda Shan shows highly comparable topographic features (e.g. occurrence of elevated planation surfaces) and thermal histories (e.g. generally slow to moderate cooling during the Meso-Cenozoic) with the Chinese Central Tianshan.

Highlights

- No Cenozoic basement AFT ages have been detected from the Bogda Shan.
- Middle Jurassic strata in the southern Junggar Basin were not buried deeply enough to completely reset their AFT clock as previously considered.
- The Bogda Shan shows highly comparable topographic features and thermal histories with the Chinese Central Tianshan.

Acknowledgments

We would like to thank three anonymous reviewers for their constructive and insightful comments, and Editor-in-Chief Prof. Robert J. Stern for his efficient editorial handling. We appreciate the help provided by Dr Bart Van Houdt and Dr Guido Vittiglio with irradiation at the Belgian Nuclear Research Centre in Mol (SCK-CEN, BR1 facility). This work is partly supported by the National Key R&D Plan of China (grants 2017YFC0601402 and 2018YFC0603703). China Scholarship Council (201806190214; 201908320260) provided financial support for Z. He and W. Su for their research stay in Belgium. S. Glorie was supported by an Australian Research Council Future Fellowship (FT210100906).

Disclosure statement

The authors declare that they have no known competing financial interests or personal relationships that could have appeared to influence the work reported in this paper.

Funding

This work is partly supported by the National Key R&D Plan of China (grants 2017YFC0601402 and 2018YFC0603703).

ORCID

Zhiyuan He  <http://orcid.org/0000-0002-5169-5557>

References

- Alexeiev, D.V., Biske, Y.S., Wang, B., Djenchuraeva, A.V., Getman, O.F., Aristov, V.A., Kröner, A., Liu, H.S., and Zhong, L.L., 2015, Tectono-stratigraphic framework and palaeozoic evolution of the Chinese South Tianshan: *Geotectonics*, v. 49, no. 2, p. 93–122. Doi:[10.1134/S0016852115020028](https://doi.org/10.1134/S0016852115020028)
- Allen, M.B., Sengör, A.M.C., and Natal'in, B.A., 1995, Junggar, Turfan and Alakol basins as Late Permian to ?Early Triassic extensional structures in a sinistral shear zone in the Altai orogenic collage, Central Asia: *Journal of Geological Society*, v. 152, no. 2, p. 327–338. Doi:[10.1144/gsjgs.152.2.0327](https://doi.org/10.1144/gsjgs.152.2.0327)
- Allen, M.B., Windley, B.F., and Zhang, C., 1992, Palaeozoic collisional tectonics and magmatism of the Chinese Tien Shan, Central Asia: *Tectonophysics*, v. 220, no. 1–4, p. 89–115. Doi:[10.1016/0040-1951\(93\)90225-9](https://doi.org/10.1016/0040-1951(93)90225-9)
- Bande, A., Sobel, E.R., Mikolaichuk, A., Schmidt, A., and Stockli, D.F., 2017, Exhumation history of the western Kyrgyz Tien Shan: Implications for intramontane basin formation: *Tectonics*, v. 36, no. 1, p. 163–180. Doi:[10.1002/2016TC004284](https://doi.org/10.1002/2016TC004284)
- Barbarand, J., Hurford, A.J., and Carter, A., 2003, Variation in apatite fission-track length measurement: Implications for thermal history modelling: *Chemical Geology*, v. 198, no. 1–2, p. 77–106. Doi:[10.1016/S0009-2541\(02\)00423-0](https://doi.org/10.1016/S0009-2541(02)00423-0)
- Burchfiel, B.C., Brown, E.T., Deng, Q.D., Feng, X.Y., Li, J., Molnar, P., Shi, J.B., Wu, Z.M., and You, H.C., 1999, Crustal shortening on the margins of the Tien Shan, Xinjiang, China: *International Geology Review*, v. 41, no. 8, p. 665–700. Doi:[10.1080/00206819909465164](https://doi.org/10.1080/00206819909465164)
- Carroll, A., Graham, S., Hendrix, M., Ying, D., and Zhou, D., 1995, Late Paleozoic tectonic amalgamation of northwestern China: Sedimentary record of the northern Tarim, northwestern Turpan, and southern Junggar basins: *Geological Society of America Bulletin*, v. 107, no. 5, p. 571–594. Doi:[10.1130/0016-7606\(1995\)107<0571:LPTAON>2.3.CO;2](https://doi.org/10.1130/0016-7606(1995)107<0571:LPTAON>2.3.CO;2)
- Chang, J., Glorie, S., Qiu, N., Min, K., Xiao, Y., and Xu, W., 2021, Late Miocene (10.0~6.0 Ma) rapid exhumation of the Chinese South Tianshan: Implications for the timing of aridification in the Tarim Basin: *Geophysical Research Letters*, v. 48, no. 3, p. e2020GL090623. Doi:[10.1029/2020GL090623](https://doi.org/10.1029/2020GL090623)
- Chang, J., Li, D., Min, K., Qiu, N.S., Xiao, Y., Wu, H., and Liu, N., 2019, Cenozoic deformation of the Kalpin fold-and-thrust belt, southern Chinese Tian Shan: New insights from low-T thermochronology and sandbox modeling: *Tectonophysics*, v. 766, p. 416–432. Doi:[10.1016/j.tecto.2019.06.018](https://doi.org/10.1016/j.tecto.2019.06.018)
- Chang, J., Qiu, N., and Li, J., 2012, Tectono-thermal evolution of the northwestern edge of the Tarim Basin in China: Constraints from apatite (U-Th)/He thermochronology:



- Journal of Asian Earth Sciences, v. 61, p. 187–198. Doi:[10.1016/j.jseaes.2012.09.020](https://doi.org/10.1016/j.jseaes.2012.09.020)
- Chang, J., Tian, Y.T., and Qiu, N.S., 2017, Mid-late Miocene deformation of the northern Kuqa fold-and-thrust belt (southern Chinese Tian Shan): An apatite (U-Th-Sm)/He study: *Tectonophysics*, v. 694, p. 101–113. Doi:[10.1016/j.tecto.2016.12.003](https://doi.org/10.1016/j.tecto.2016.12.003)
- Charvet, J., Shu, L.S., and Laurent-Charvet, S., 2007, Paleozoic structural and geodynamic evolution of eastern Tianshan (NW China): Welding of the Tarim and Junggar plates: *Episodes*, v. 30, p. 162–186
- Charvet, J., Shu, L.S., Laurent-Charvet, S., Wang, B., Faure, M., Cluzel, D., Chen, Y., and Jong, K., 2011, Palaeozoic tectonic evolution of the Tianshan belt: NW China: *Science China Earth Sciences*, v. 54, p. 166–184. Doi:[10.1007/s11430-010-4138-1](https://doi.org/10.1007/s11430-010-4138-1)
- Chen, X., Shu, L., and Santosh, M., 2011, Late Paleozoic post-collisional magmatism in the Eastern Tianshan Belt, Northwest China: New insights from geochemistry, geochronology and petrology of bimodal volcanic rocks: *Lithos*, v. 127, no. 3–4, p. 581–598. Doi:[10.1016/j.lithos.2011.06.008](https://doi.org/10.1016/j.lithos.2011.06.008)
- Chen, X., Shu, L., Santosh, M., and Zhao, X., 2013, Island arc-type bimodal magmatism in the eastern Tianshan Belt, Northwest China: Geochemistry, zircon U-Pb geochronology and implications for the Paleozoic crustal evolution in Central Asia: *Lithos*, v. v, p. 168–169. Doi:[10.1016/j.lithos.2012.10.006](https://doi.org/10.1016/j.lithos.2012.10.006)
- Chen, Y., Wang, G.C., Kapp, P., Shen, T.Y., Zhang, P., Zhu, C.Y., and Cao, K., 2020a, Episodic exhumation and related tectonic controlling during Mesozoic in the Eastern Tian Shan, Xinjiang, northwestern China: *Tectonophysics*, v. 796, p. 228647. Doi:[10.1016/j.tecto.2020.228647](https://doi.org/10.1016/j.tecto.2020.228647)
- Chen, Y., Wang, G.C., Shen, T.Y., Zhang, P., Sotirious, P., and Zhu, C.Y., 2020b, Tectono-geomorphic evolution of Harlik Mountain in the Eastern Tian Shan, insight from thermo-chronological data and geomorphic analysis: *Geological Journal*, v. 55, no. 11, p. 7322–7334. Doi:[10.1002/gj.3951](https://doi.org/10.1002/gj.3951)
- Chen, D.C., Zhao, X.M., and Deng, J., 2010, U-Pb dating of Carboniferous sandstone detrital zircon from the north of the Bogda Mountains, eastern Xinjiang, and its geological significances: *Acta Geologica Sinica*, v. 84, p. 1770–1780. in Chinese with English abstract
- Cunningham, D., 2021, Tectonic Geomorphology of Intracontinental Mountain Ranges: Treatise on Geomorphology, Second, Vol. 2 (Elsevier), p. 198–222. Doi:[10.1016/B978-0-12-818234-5.00091-2](https://doi.org/10.1016/B978-0-12-818234-5.00091-2)
- Cunningham, D., Owen, L.A., Snee, L., and Li, J., 2003, Structural framework of a major intracontinental orogenic termination zone: The easternmost Tien Shan, China: *Journal of Geological Society*, v. 160, no. 3, p. 575–590. Doi:[10.1144/0016-764902-122](https://doi.org/10.1144/0016-764902-122)
- De Corte, F., Bellemans, F., Van den Haute, P., Ingelbrecht, C., and Nicholl, C., 1998, A new U doped glass certified by the European Commission for the calibration of fission-track dating, in Van den Haute, P., and De Corte, F., eds., *Advances in Fission-track Geochronology*. Kluwer Academic Publishers, Dordrecht. p. 67–78. Doi:[10.1007/978-94-015-9133-1_5](https://doi.org/10.1007/978-94-015-9133-1_5)
- De Grave, J., Buslov, M.M., and Van den Haute, P., 2007, Distant effects of India-Eurasia convergence and Mesozoic intracontinental deformation in Central Asia: Constraints from apatite fission-track thermochronology: *Journal of Asian Earth Sciences*, v. 29, no. 2–3, p. 188–204. Doi:[10.1016/j.jseaes.2006.03.001](https://doi.org/10.1016/j.jseaes.2006.03.001)
- De Grave, J., Glorie, S., Buslov, M.M., Izmer, A., Fournier-Carrie, A., Batalev, V.Y., Vanhaecke, F., Elburg, M.A., and Van den Haute, P., 2011, The thermo-tectonic history of the Song-Kul Plateau, Kyrgyz Tien Shan: Constraints by apatite and titanite thermochronometry and zircon U/Pb dating: *Gondwana Research*, v. 20, no. 4, p. 745–763. Doi:[10.1016/j.gr.2011.03.011](https://doi.org/10.1016/j.gr.2011.03.011)
- De Grave, J., Glorie, S., Buslov, M.M., Stockli, D.F., McWilliams, M.O., Batalev, V.Y., and Van den Haute, P., 2013, Thermo-tectonic history of the Issyk-kul basement (Kyrgyz northern Tien Shan, Central Asia): *Gondwana Research*, v. 23, no. 3, p. 998–1020. Doi:[10.1016/j.gr.2012.06.014](https://doi.org/10.1016/j.gr.2012.06.014)
- De Grave, J., Glorie, S., Ryabinin, A., Zhimulev, F., Buslov, M.M., Izmer, A., Elburg, M., Vanhaecke, F., and Van den Haute, P., 2012, Late Palaeozoic and Meso-Cenozoic tectonic evolution of the southern Kyrgyz Tien Shan: Constraints from multi-method thermochronology in the Trans-Alai, Turkestan-Alai segment and the southeastern Ferghana Basin: *Journal of Asian Earth Sciences*, v. 44, p. 149–168. Doi:[10.1016/j.jseaes.2011.04.019](https://doi.org/10.1016/j.jseaes.2011.04.019)
- De Grave, J., Glorie, S., Vermaercke, P., Vittiglio, G., and Van den Haute, P., 2010, A “new” irradiation facility for FT applications at the Belgian Nuclear Research Centre: The BR1 reactor. Abstract, Thermo 2010, 12th International Conference on Thermochronology Glasgow, United Kingdom, p. 119.
- Donelick, R.A., and Miller, D.S., 1991, Enhanced tint fission track densities in low spontaneous track density apatites using ^{252}Cf -derived fission fragment tracks: A model and experimental observations: *International Journal of Radiation Applications and Instrumentation. Part D. Nuclear Tracks and Radiation Measurements*, v. 18, no. 3, p. 301–307. Doi:[10.1016/1359-0189\(91\)90022-A](https://doi.org/10.1016/1359-0189(91)90022-A)
- Dumitru, T.A., Zhou, D., Chang, E.Z., and Graham, S.A., 2001, Uplift, exhumation, and deformation in the Chinese Tian Shan: *Geological Society of America: Memoir*, v. 194, p. 71–99. Doi:[10.1130/0-8137-1194-0.71](https://doi.org/10.1130/0-8137-1194-0.71)
- Fang, Y.N., Wu, C.D., Wang, Y.Z., Hou, K.L., and Guo, Z.J., 2019, Topographic evolution of the Tianshan Range and their relation to the Junggar and Turpan Basins, Central Asia, from the Permian to the Neogene: *Gondwana Research*, v. 75, p. 47–67. Doi:[10.1016/j.gr.2019.03.020](https://doi.org/10.1016/j.gr.2019.03.020)
- Fernie, N., Glorie, S., Jessell, M.W., and Collins, A.S., 2018, Thermochronological insights into reactivation of a continental shear zone in response to Equatorial Atlantic rifting (northern Ghana: *Scientific Reports*, v. 8, no. 1, p. 16619. Doi:[10.1038/s41598-018-34769-x](https://doi.org/10.1038/s41598-018-34769-x)
- Galbraith, R.F., and Green, P.F., 1990, Estimating the component ages in a finite mixture: *International Journal of Radiation Applications and Instrumentation. Part D. Nuclear Tracks and Radiation Measurements*, v. 17, no. 3, p. 197–206. Doi:[10.1016/1359-0189\(90\)90035-V](https://doi.org/10.1016/1359-0189(90)90035-V)
- Gallagher, K., 2012, Transdimensional inverse thermal history modeling for quantitative thermochronology: *Journal of Geophysical Research*, v. 117, no. B2, p. B02408. Doi:[10.1029/2011JB008825](https://doi.org/10.1029/2011JB008825)
- Gallagher, K., Charvin, K., Nielsen, S., Sambridge, M., and Stephenson, J., 2009, Markov chain Monte Carlo (MCMC) sampling methods to determine optimal models, model resolution and model choice for Earth Science problems:

- Marine and Petroleum Geology, v. 26, no. 4, p. 525–535. Doi:[10.1016/j.marpetgeo.2009.01.003](https://doi.org/10.1016/j.marpetgeo.2009.01.003)
- Gao, J., Klemd, R., Qian, Q., Zhang, X., Li, J., Jiang, T., and Yang, Y. Q., 2011, The collision between the Yili and Tarim blocks of the Southwestern Altaiids: Geochemical and age constraints of a leucogranite dike crosscutting the HP-LT metamorphic belt in the Chinese Tianshan Orogen: *Tectonophysics*, v. 499, no. 1–4, p. 118–131. Doi:[10.1016/j.tecto.2011.01.001](https://doi.org/10.1016/j.tecto.2011.01.001)
- Gao, J.G., Li, W.Y., Liu, J.C., Gao, Y.X., Guo, X.C., Zhou, Y., and Fan, T.B., 2014, Geochemistry, zircon U-Pb age and Hf isotopes of late Carboniferous rift volcanic in the Sepikou region, eastern Bogda, Xinjiang: *Acta Petrologica Sinica*, v. 30, p. 3539–3552. in Chinese with English abstract
- Gao, J., Li, M.S., Xiao, X.C., Tang, Y.Q., and He, G.Q., 1998, Paleozoic tectonic evolution of the Tianshan Orogen, northwestern China: *Tectonophysics*, v. 287, no. 1–4, p. 213–231. Doi:[10.1016/S0040-1951\(98\)80070-X](https://doi.org/10.1016/S0040-1951(98)80070-X)
- Gillespie, J., Glorie, S., Jepson, G., Xiao, W., and Collins, A.S., 2020, Late Paleozoic exhumation of the West Junggar Mountains: NW China: *Journal of Geophysical Research: Solid Earth*, v. 125, p. e2019JB018013. Doi:[10.1029/2019JB018013](https://doi.org/10.1029/2019JB018013)
- Gillespie, J., Glorie, S., Jepson, G., Zhang, Z.Y., Xiao, W.J., Danišík, M., and Collins, A.S., 2017a, Differential exhumation and crustal tilting in the easternmost Tianshan (Xinjiang, China), revealed by low-temperature thermochronology: *Tectonics*, v. 36, no. 10, p. 2142–2158. Doi:[10.1002/2017TC004574](https://doi.org/10.1002/2017TC004574)
- Gillespie, J., Glorie, S., Jepson, G., Zhimulev, F., Gurevich, D., Danišík, M., and Collins, A.S., 2021, Inherited structure as a control on late Paleozoic and Mesozoic exhumation of the Tarbagatai Mountains, southeastern Kazakhstan: *Journal of the Geological Society*, v. 178, no. 6, p. jgs2020–121. Doi:[10.1144/jgs2020-121](https://doi.org/10.1144/jgs2020-121)
- Gillespie, J., Glorie, S., Xiao, W.J., Zhang, Z.Y., Collins, A.S., Evans, N., McInnes, B., and De Grave, J., 2017b, Mesozoic reactivation of the Beishan, southern Central Asian Orogenic Belt: Insights from low-temperature thermochronology: *Gondwana Research*, v. 43, p. 107–122. Doi: [10.1016/j.gr.2015.10.004](https://doi.org/10.1016/j.gr.2015.10.004)
- Glorie, S., and De Grave, J., 2016, Exhuming the Meso-Cenozoic Kyrgyz Tianshan and Siberian Altai-Sayan: A review based on low-temperature thermochronology: *Geoscience Frontiers*, v. 7, no. 2, p. 155–170. Doi:[10.1016/j.gsf.2015.04.003](https://doi.org/10.1016/j.gsf.2015.04.003)
- Glorie, S., De Grave, J., Buslov, M.M., Elburg, M.A., Stockli, D.F., Gerdes, A., and Van den Haute, P., 2010, Multi-method chronometric constraints on the evolution of the Northern Kyrgyz Tien Shan granitoids (Central Asian Orogenic Belt): From emplacement to exhumation: *Journal of Asian Earth Sciences*, v. 38, no. 3–4, p. 131–146. Doi:[10.1016/j.jseas.2009.12.009](https://doi.org/10.1016/j.jseas.2009.12.009)
- Glorie, S., De Grave, J., Buslov, M.M., Zhimulev, F.I., Stockli, D.F., Batalev, V.Y., Izmer, A., Van den Haute, P., Vanhaecke, F., and Elburg, M., 2011, Tectonic history of the Kyrgyz South Tien Shan (Atbashi-Inylchek) suture zone: The role of inherited structures during deformation-propagation: *Tectonics*, v. 30, no. 6, p. TC6016. [10.1029/2011TC002949](https://doi.org/10.1029/2011TC002949)
- Glorie, S., Otasevic, A., Gillespie, J., Jepson, G., Danišík, M., Zhimulev, F.I., Gurevich, G., Zhang, Z., Song, D., and Xiao, W., 2019, Thermo-tectonic history of the junggar alatau within the central asian orogenic belt (SE Kazakhstan, NW China): Insights from integrated apatite U/Pb, fission track and (U-Th)/He thermochronology: *Geoscience Frontiers*, v. 10, no. 6, p. 2153–2166. [10.1016/j.gsf.2019.05.005](https://doi.org/10.1016/j.gsf.2019.05.005)
- Greene, T.J., Carroll, A.R., Wartes, M., Graham, S.A., and Wooden, J.L., 2005, Integrated provenance analysis of a complex orogenic terrane: Mesozoic uplift of the Bogda Shan and inception of the Turpan-Hami Basin: NW China: *Journal of Sedimentary Research*, v. 75, p. 251–267. [10.2110/jsr.2005.019](https://doi.org/10.2110/jsr.2005.019)
- Gu, L., Hu, S., Yu, C., Li, H., Xiao, X., and Yan, Z., 2000, Carboniferous volcanites in the Bogda orogenic belt of eastern Tianshan: Their tectonic implications: *Acta Petrologica Sinica*, v. 16, p. 305–316. in Chinese with English abstract
- Han, B.F., Guo, Z.J., Zhang, Z.C., Zheng, L., Chen, J.F., and Song, B., 2010, Age, geochemistry, and tectonic implications of a late Paleozoic stitching pluton in the North Tian Shan suture zone, western China: *Geological Society of America Bulletin*, v. 122, no. 3–4, p. 627–640. [10.1130/B26491.1](https://doi.org/10.1130/B26491.1)
- Han, B.F., He, G.Q., Wang, X.C., and Guo, Z.J., 2011, Late Carboniferous collision between the Tarim and Kazakhstan-Yili terranes in the western segment of the South Tian Shan Orogen, Central Asia, and implications for the Northern Xinjiang, western China: *Earth-Science Reviews*, v. 109, no. 3–4, p. 74–93. [10.1016/j.earscirev.2011.09.001](https://doi.org/10.1016/j.earscirev.2011.09.001)
- Han, Y.G., and Zhao, G.C., 2018, Final amalgamation of the Tianshan and Junggar orogenic collage in the southwestern Central Asian Orogenic Belt: Constraints on the closure of the Paleo-Asian Ocean: *Earth-Science Reviews*, v. 186, p. 129–152. [10.1016/j.earscirev.2017.09.012](https://doi.org/10.1016/j.earscirev.2017.09.012)
- Han, Y.G., Zhao, G.C., Sun, M., Eizenhöfer, P.R., Hou, W.Z., Zhang, X.R., Liu, D.X., Wang, B., and Zhang, G.W., 2015, Paleozoic accretionary orogenesis in the Paleo-Asian Ocean: Insights from detrital zircons from Silurian to Carboniferous strata at the northwestern margin of the Tarim Craton: *Tectonics*, v. 34, no. 2, p. 334–351. [10.1002/2014TC003668](https://doi.org/10.1002/2014TC003668)
- He, Z.Y., 2022, Intra-continental evolution of the Chinese Tianshan and Junggar orogenic collage. Ghent University, PhD thesis, p. 1–314.
- Hendriks, B.W.H., and Redfeld, T.F., 2005, Apatite fission track and (U-Th)/He data from Fennoscandia: An example of underestimation of fission track annealing in apatite: *Earth and Planetary Science Letters*, v. 236, no. 1–2, p. 443–458. [10.1016/j.epsl.2005.05.027](https://doi.org/10.1016/j.epsl.2005.05.027)
- Hendrix, M.S., Brassell, S.C., Carroll, A.R., and Graham, S.A., 1995, Sedimentology, Organic Geochemistry, and Petroleum Potential of Jurassic Coal Measures: Tarim, Junggar, and Turpan Basins, Northwest China: *AAPG Bulletin V*, v. 79, no. 7, p. 929–958. [10.1306/8D2B2187-171E-11D7-8645000102C1865D](https://doi.org/10.1306/8D2B2187-171E-11D7-8645000102C1865D)
- Hendrix, M.S., Graham, S.A., Carroll, A.R., Sober, E.R., McKnight, C. L., Shulein, B.J., and Wang, Z.X., 1992, Sedimentary record and climatic implications of recurrent deformation of the Tien Shan: Evidence from Mesozoic strata of the North Tarim, South Junggar and Turpan basins: *Geological Society of America Bulletin*, v. 104, no. 1, p. 53–79. [10.1130/0016-7606\(1992\)104<0053:SRACIO>2.3.CO;2](https://doi.org/10.1130/0016-7606(1992)104<0053:SRACIO>2.3.CO;2)
- He, Z.Y., Wang, B., Glorie, S., Su, W.B., Ni, X.H., Jepson, G., Liu, J.S., Zhong, L.L., Gillespie, J., and De Grave, J., 2022a, Mesozoic building of the Eastern Tianshan and East Junggar (NW China) revealed by low-temperature thermochronology: *Gondwana Research*, v. 103, p. 37–53. [10.1016/j.gr.2021.11.013](https://doi.org/10.1016/j.gr.2021.11.013)



- He, Z.Y., Wang, B., Nachtergaelie, S., Glorie, S., Ni, X.H., Su, W.B., Cai, D.X., Liu, J.S., and De Grave, J., [2021b](#), Long-term topographic evolution of the Central Tianshan (NW China) constrained by low-temperature thermochronology: *Tectonophysics*, v. 817, p. 229066. [10.1016/j.tecto.2021.229066](#)
- He, Z.Y., Wang, B., Ni, X.H., De Grave, J., Scaillet, S., Chen, Y., Liu, J.S., and Zhu, X., [2021a](#), Structural and kinematic evolution of strike-slip shear zones around and in the Central Tianshan: Insights for eastward tectonic wedging in the southwest Central Asian Orogenic Belt: *Journal of Structural Geology*, v. 144, p. 104279. [10.1016/j.jsg.2021.104279](#)
- He, Z.Y., Wang, B., Su, W.B., Glorie, S., Ni, X.H., Liu, J.S., Cai, D.X., Zhong, L.L., and De Grave, J., [2022b](#), Mesozoic thermo-tectonic evolution of the Yili block within the Central Asian Orogenic Belt (NW China): Insights from apatite fission track thermochronology: *Tectonophysics*, v. 823, p. 229194. [10.1016/j.tecto.2021.229194](#)
- He, Z.Y., Wang, B., Zhong, L.L., and Zhu, X.Y., [2018](#), Crustal evolution of the Central Tianshan Block: Insights from zircon U-Pb isotopic and structural data from meta-sedimentary and meta-igneous rocks along the Wulasitai - Wulanmoren shear zone: *Precambrian Research*, v. 314, p. 111–128. [10.1016/j.precamres.2018.06.003](#)
- Huang, B., Piper, J., Peng, S., Liu, T., Li, Z., Wang, Q., and Zhu, R., [2006](#), Magnetostriatigraphic study of the Kuche Depression, Tarim Basin, and Cenozoic uplift of the Tian Shan Range, Western China: *Earth and Planetary Science Letters*, v. 251, no. 3–4, p. 346–364. [10.1016/j.epsl.2006.09.020](#)
- Hubert-Ferrari, A., Suppe, J., Gonzalez-Mieres, R., and Wang, X., [2007](#), Mechanisms of active folding of the landscape (southern Tian Shan, China): *Journal of Geophysical Research*, v. 112, no. B3, p. B03S09. [10.1029/2006JB004362](#)
- Hurford, A.J., [1990](#), Standardization of fission track dating calibration: Recommendation by the Fission Track Working Group of the I.U.G.S. Subcommission on Geochronology: *Chemical Geology: Isotope Geoscience Section*, v. 80, p. 171–178. [10.1016/0168-9622\(90\)90025-8](#)
- Hurford, A.J., and Hammerschmidt, K., [1985](#), $^{40}\text{Ar}/^{39}\text{Ar}$ and K/Ar dating of the Bishop and Fish Canyon Tuffs: Calibration ages for fission-track dating standards: *Chemical Geology*, v. 58, no. 1–2, p. 23–32. [10.1016/0168-9622\(85\)90024-7](#)
- Jepson, G., Glorie, S., Khudoley, A.K., Malyshov, S.V., Gillespie, J., Glasbacher, U.A., Carrapa, B., Soloviev, A.V., and Collins, A.S., [2021](#), The Mesozoic exhumation history of the Karatau-Talas range, western Tian Shan, Kazakhstan-Kyrgyzstan: *Tectonophysics*, v. 814, p. 228977. [10.1016/j.tecto.2021.228977](#)
- Jepson, G., Glorie, S., Konopelko, D., Gillespie, J., Danisik, M., Evans, N.J., Mamadjanov, Y., and Collins, A.S., [2018b](#), Thermochronological insights into the structural contact between the Tian Shan and Pamirs, Tajikistan: *Terra Nova*, V, v. 30, no. 2, p. 95–104. [10.1111/ter.12313](#)
- Jepson, G., Glorie, S., Konopelko, D., Gillespie, J., Danisik, M., Mirkamalov, R., Mamadjanov, Y., and Collins, A.S., [2018a](#), Low-temperature thermochronology of the Chatkal-Kurama terrane (Uzbekistan-Tajikistan): Insights into the Meso-Cenozoic thermal history of the western Tian Shan: *Tectonics*, v. 37, no. 10, p. 3954–3969. [10.1029/2017TC004878](#)
- Jiao, R.H., Yuan, X.P., Braun, J., and Wang, Z.X., [2021](#), Thermo-kinematic modeling of the Cenozoic uplift of the Bogda Shan: Northwest China: *Tectonophysics*, v. 816, p. 229031. [10.1016/j.tecto.2021.229031](#)
- Ji, H., Tao, H., Wang, Q., Qiu, Z., Ma, D., Qiu, J., and Liao, P., [2018](#), Early to Middle Jurassic tectonic evolution of the Bogda Mountains, Northwest China: Evidence from sedimentology and detrital zircon geochronology: *Journal of Asian Earth Sciences*, v. 153, p. 57–74. [10.1016/j.jseaes.2017.03.018](#)
- Jolivet, M., Dominguez, S., Charreau, J., Chen, Y., Li, Y., and Wang, Q., [2010](#), Mesozoic and Cenozoic tectonic history of the central Chinese Tian Shan: Reactivated tectonic structures and active deformation: *Tectonics*, v. 29, no. 6, p. TC6019. [10.1029/2010TC002712](#)
- Jolivet, M., Heilbronn, G., Robin, C., Barrier, L., Bourquin, S., Guo, Z., Jia, Y., Guerit, L., Yang, W., and Fu, B., [2013](#), Reconstructing the Late Palaeozoic-Mesozoic topographic evolution of the Chinese Tian Shan: Available data and remaining uncertainties: *Advances in Geosciences*, v. 37, p. 7–18. [10.5194/adgeo-37-7-2013](#)
- Käßner, A., Ratschbacher, L., Pfänder, J.A., Hacker, B.R., Zack, G., Sonntag, B.L., Khan, J., Stanek, K.P., Gadoev, M., and Oimahmadov, I., [2017](#), Proterozoic–Mesozoic history of the Central Asian orogenic belt in the Tajik and southwestern Kyrgyz Tian Shan: U-Pb, 40 Ar/ 39 Ar, and fission-track geochronology and geochemistry of granitoids: *Geological Society of America Bulletin*, v. 129, no. 3–4, p. 281–303. [10.1130/B31466.1](#)
- Ketcham, R.A., Carter, A., Donelick, R.A., Barbarand, J., and Hurford, A.J., [2007](#), Improved modeling of fission-track annealing in apatite: *American Mineralogist*, v. 92, no. 5–6, p. 799–810. [10.2138/am.2007.2281](#)
- Ketcham, R.A., Donelick, R.A., and Carlson, W.D., [1999](#), Variability of apatite fission-track annealing kinetics: III. Extrapolation to geological time scales: *American Mineralogist*, v. 84, no. 9, p. 1235–1255. [10.2138/am-1999-0903](#)
- Kröner, A., Kovach, V., Belousova, E., Hegner, E., Armstrong, R., Dolgopolova, A., Seltmann, R., Alexeiev, D.V., Hoffmann, J.E., Wong, J., Sun, M., Cai, K., Wang, T., Tong, Y., Wilde, S.A., Degtyarev, K.E., and Rytsk, E., [2014](#), Reassessment of continental growth during the accretionary history of the Central Asian Orogenic Belt: *Gondwana Research*, v. 25, no. 1, p. 103–125. [10.1016/j.gr.2012.12.023](#)
- Macaulay, E.A., Sobel, E.R., Mikolaichuk, A., Kohn, B., and Stuart, F.M., [2014](#), Cenozoic deformation and exhumation history of the Central Kyrgyz Tien Shan: *Tectonics*, v. 33, no. 2, p. 135–165. [10.1002/2013TC003376](#)
- Macaulay, E.A., Sobel, E.R., Mikolaichuk, A., Landgraf, A., Kohn, B., and Stuart, F., [2013](#), Thermochronologic insight into late Cenozoic deformation in the basement-cored Terskey Range Kyrgyz Tien Shan: *Tectonics*, v. 32, no. 3, p. 487–500. [10.1002/tect.20040](#)
- Malusà, M.G., and Fitzgerald, P.G., [2019](#), *Fission-Track Thermochronology and its Application to Geology*, Berlin/Heidelberg, Germany: Springer, p. 1–393. [10.1007/978-3-319-89421-8](#)
- Ma, R., Shu, L., and Sun, J., [1997](#), *Tectonic Evolution and Metallization in the Eastern Tianshan Belt*, Geological Publishing House, Beijing, p. 1–202. in Chinese
- McDowell, F.W., McIntosh, W.C., and Farley, K.A., [2005](#), A precise $^{40}\text{Ar}/^{39}\text{Ar}$ reference age for the Durango apatite (U-Th)/He and fission-track dating standard: *Chemical*

- Geology, v. 214, no. 3–4, p. 249–263. [10.1016/j.chemgeo.2004.10.002](https://doi.org/10.1016/j.chemgeo.2004.10.002)
- Molnar, P., and Tapponnier, P., **1975**, Cenozoic tectonics of Asia: Effects of a continental collision: *Science*, v. 189, p. 419–426
- Morin, J., Jolivet, M., Barrier, L., Laborde, A., Li, H.B., and Dauteuil, O., **2019**, Planation surfaces of the Tian Shan Range (Central Asia): Insight on several 100 million years of topographic evolution: *Journal of Asian Earth Sciences*, v. 177, p. 52–65. [10.1016/j.jseaes.2019.03.011](https://doi.org/10.1016/j.jseaes.2019.03.011)
- Mossakovskiy, A.A., Ruzhentsev, S.V., Samygin, S.G., and Kheraskova, T.N., **1993**, Central Asian fold belt: Geodynamic evolution and history of formation: *Geotectonics*, v. 6, p. 3–33
- Nachtergaelie, S., De Pelsmaeker, E., Glorie, S., Zhimulev, F., Jolivet, M., Danišik, M., Buslov, M.M., and De Grave, J., **2018**, Meso-Cenozoic tectonic evolution of the Talas-Fergana Region of the Kyrgyz Tien Shan revealed by low-temperature basement and detrital thermochronology: *Geoscience Frontiers*, v. 9, no. 5, p. 1495–1514. [10.1016/j.gsf.2017.11.007](https://doi.org/10.1016/j.gsf.2017.11.007)
- Ni, X.H., Wang, B., Cruzel, D., Liu, L.S., and He, Z.Y., **2021**, Late Paleozoic tectonic evolution of the North Tianshan Belt: New structural and geochronological constraints from meta-sedimentary rocks and migmatites in the Harlik Range (NW China): *Journal of Asian Earth Sciences*, v. 210, p. 104711. [10.1016/j.jseaes.2021.104711](https://doi.org/10.1016/j.jseaes.2021.104711)
- Qian, Q., Gao, J., Klemd, R., He, G.Q., Song, B., Liu, D.Y., and Xu, R. H., **2009**, Early Paleozoic tectonic evolution of the Chinese South Tianshan Orogen: Constraints from SHRIMP zircon U-Pb geochronology and geochemistry of basaltic and dioritic rocks from Xiate, NW China: *International Journal of Earth Sciences*, v. 98, no. 3, p. 551–569. [10.1007/s00531-007-0268-x](https://doi.org/10.1007/s00531-007-0268-x)
- Şengör, A.M.C., Natal'in, B.A., and Burtman, V.S., **1993**, Evolution of the Altaiid tectonic collage and Palaeozoic crustal growth in Eurasia: *Nature*, v. 364, no. 6435, p. 299–307. [10.1007/s00531-007-0268-x](https://doi.org/10.1007/s00531-007-0268-x)
- Shen, T., Chen, Y., Wang, G., Ji, J., Wang, Y., Zhang, P., Sotiriou, P., Guo, R., and Xu, Z., **2020**, Detrital zircon geochronology analysis of the late Mesozoic deposition in the Turpan-Hami basin: Implications for the uplift history of the Eastern Tian Shan, North-Western China: *Terra Nova*, v. 32, no. 2, p. 166–178. [10.1111/ter.12445](https://doi.org/10.1111/ter.12445)
- Shen, C.B., Mei, L.F., Liu, L., Tang, J.G., and Zhou, F., **2005**, Characteristics of fission track age of Bogedashan in Xinjiang and its structural significance: *Journal of Oil and Gas Technology*, v. 27, p. 273–276. in Chinese with English abstract
- Shu, L.S., Wang, B., Zhu, W.B., Guo, Z.J., Charvet, J., and Zhang, Y., **2011**, Timing of initiation of extension in the Tianshan, based on structural, geochemical and geochronological analyses of bimodal volcanism and olistostrome in the Bogda Shan (NW China): *International Journal of Earth Sciences*, v. 100, no. 7, p. 1647–1663. [10.1007/s00531-010-0575-5](https://doi.org/10.1007/s00531-010-0575-5)
- Shu, L., Zhu, W., Wang, B., Faure, M., Charvet, J., and Cluzel, D., **2005**, The post-collision intracontinental rifting and olistostrome on the southern slope of Bogda Mountains, Xinjiang: *Acta Petrologica Sinica*, v. 21, p. 25–36. in Chinese with English abstract
- Sun, J.B., Chen, W., Qin, K.Z., Danišik, M., Evans, N.J., McInnes, B. I.A., Shen, Z., Zhao, S.F., Zhang, B., Yin, J.Y., and Tao, N., **2021**, Mesozoic exhumation of the Jueluotage area, Eastern Tianshan, NW China: Constraints from (U-Th)/He and fission-track thermochronology: *Geological Magazine*, v. 158, no. 11, p. 1960–1976. [10.1017/S0016756821000522](https://doi.org/10.1017/S0016756821000522)
- Tang, W., Zhang, Z., Li, J., Li, K., Chen, Y., and Guo, Z., **2014**, Late Paleozoic to Jurassic tectonic evolution of the Bogda area (northwest China): Evidence from detrital zircon U-Pb geochronology: *Tectonophysics*, v. 626, p. 144–156. [10.1016/j.tecto.2014.04.005](https://doi.org/10.1016/j.tecto.2014.04.005)
- Tang, W., Zhang, Z., Li, J., Li, K., Luo, Z., and Chen, Y., **2015**, Mesozoic and Cenozoic uplift and exhumation of the Bogda Mountain, NW China: Evidence from apatite fission track analysis: *Geoscience Frontiers*, v. 6, no. 4, p. 617–625. [10.1016/j.gsf.2014.04.006](https://doi.org/10.1016/j.gsf.2014.04.006)
- Van Ranst, G., Baert, P., Fernandes, A.C., and De Grave, J., **2020**, Technical note: Nikon-TRACKFlow, a new versatile microscope system for fission track analysis: *Geochronology*, v. 2, no. 1, p. 93–99. [10.5194/gchron-2-93-2020](https://doi.org/10.5194/gchron-2-93-2020)
- Vermeesch, P., **2009**, RadialPlotter: A Java application for fission track, luminescence and other radial plots: *Radiation Measurements*, v. 44, no. 4, p. 409–410. [10.1016/j.radmeas.2009.05.003](https://doi.org/10.1016/j.radmeas.2009.05.003)
- Vermeesch, P., **2018**, IsoplotR: A free and open toolbox for geochronology: *Geoscience Frontiers*, v. 9, no. 5, p. 1479–1493. [10.1016/j.gsf.2018.04.001](https://doi.org/10.1016/j.gsf.2018.04.001)
- Wang, Y.N., Cai, K.D., Sun, M., and Bao, Z.H., **2021**, Burial and exhumation of late paleozoic arc-related rocks in the Tulasu basin, Western Chinese Tianshan: Implication for the preservation of epithermal deposits in old orogenic belts: *Gondwana Research*, v. 97, p. 51–67. [10.1016/j.gr.2021.05.010](https://doi.org/10.1016/j.gr.2021.05.010)
- Wang, Y.N., Cai, K.D., Sun, M., Xiao, W.J., De Grave, J., Wan, B., and Bao, Z.H., **2018d**, Tracking the multi-stage exhumation history of the western Chinese Tianshan by Apatite Fission Track (AFT) dating: Implications for the preservation of epithermal deposits in the ancient orogenic belt: *Ore Geology Reviews*, v. 100, p. 111–132. [10.1016/j.oregeorev.2017.04.011](https://doi.org/10.1016/j.oregeorev.2017.04.011)
- Wang, J., Cao, Y.C., Wang, X.T., Liu, K.Y., Wang, Z.K., and Xu, Q.S., **2018a**, Sedimentological constraints on the initial uplift of the West Bogda Mountains in Mid-Permian: *Scientific Reports*, v. 8, no. 1, p. 1453. [10.1038/s41598-018-19856-3](https://doi.org/10.1038/s41598-018-19856-3)
- Wang, B., Cluzel, D., Jahn, B.-M., Shu, L., Chen, Y., Zhai, Y., Branquet, Y., Barbanson, L., and Sizaret, S., **2014b**, Late Paleozoic pre- and syn-kinematic plutons of the Kangguer-Huangshan Shear zone: Inference on the tectonic evolution of the eastern Chinese north Tianshan: *American Journal of Science*, v. 314, no. 1, p. 43–79. [10.2475/01.2014.02](https://doi.org/10.2475/01.2014.02)
- Wang, B., Faure, M., Shu, L.S., Cluzel, D., Charvet, J., de Jong, K., and Chen, Y., **2008b**, Paleozoic geodynamic evolution of the Yili Block, Western Chinese Tianshan: *Bulletin de la Société Géologique de France*, v. 179, no. 5, p. 483–490. [10.2113/gssgbull.179.5.483](https://doi.org/10.2113/gssgbull.179.5.483)
- Wang, S., Jiao, R.H., Ren, Z.K., Wu, C.Y., Ren, G.X., Zhang, H.P., and Lei, Q.Y., **2020**, Active thrusting in an intermontane basin: The Kumysh Fault, eastern Tian Shan: *Tectonics*, v. 39, no. 8, p. e2019TC006029. [10.1029/2019TC006029](https://doi.org/10.1029/2019TC006029)
- Wang, Y.J., Jia, D., Pan, J.G., Wei, D.T., Tang, Y., Wang, G.D., Wei, C.R., and Ma, D.L., **2018c**, Multiple-phase tectonic superposition and reworking in the Junggar Basin of northwestern China—Implications for deep seated petroleum exploration: *AAPG Bulletin*, v. 102, no. 8, p. 1489–1521. [10.13061/10181716518](https://doi.org/10.13061/10181716518)



- Wang, Y., Li, J.Y., and Sun, G.H., 2008c, Postcollisional Eastward Extrusion and Tectonic Exhumation along the Eastern Tianshan Orogen, Central Asia: Constraints from Dextral Strike-Slip Motion and 40 Ar/ 39 Ar Geochronological Evidence: *The Journal of Geology*, v. 116, no. 6, p. 599–618. [10.1086/591993](https://doi.org/10.1086/591993)
- Wang, B., Liu, H.S., Shu, L.S., Jahn, B.M., Chung, S.L., Zhai, Y.Z., and Liu, D.Y., 2014a, Early Neoproterozoic crustal evolution in northern Yili Block: Insights from migmatite, orthogneiss and leucogranite of the Wenquan metamorphic complex in the NW Chinese Tianshan: *Precambrian Research*, v. 242, p. 58–81. [10.1016/j.precamres.2013.12.006](https://doi.org/10.1016/j.precamres.2013.12.006)
- Wang, Z.X., Li, T., Zhang, J., Liu, Y.Q., and Ma, Z.J., 2008a, The uplifting process of the Bogda Mountain during the Cenozoic and its tectonic implication: *Science in China Series D: Earth Sciences*, v. v, p. 51. [10.1007/s11430-008-0038-z](https://doi.org/10.1007/s11430-008-0038-z)
- Wang, F.J., Luo, M., He, Z.Y., Ge, R.F., Cao, Y.Y., De Grave, J., and Zhu, W.B., 2022, Late Mesozoic intracontinental deformation and magmatism in the Chinese Tianshan and adjacent areas, Central Asia: *Geological Society of America Bulletin*, p. B36318. [10.1130/B36318.1](https://doi.org/10.1130/B36318.1)
- Wang, B., Shu, L., Faure, M., Jahn, B.M., Cluzel, D., Charvet, J., Chung, S.L., and Meffre, S., 2011, Paleozoic tectonics of the southern Chinese Tianshan: Insights from structural, chronological and geochemical studies of the Heiyingshan ophiolitic mélange (NW China): *Tectonophysics*, v. 497, no. 1–4, p. 85–104. [10.1016/j.tecto.2010.11.004](https://doi.org/10.1016/j.tecto.2010.11.004)
- Wang, X.W., Wang, X.W., and Ma, Y.S., 2007, Differential exhumation history of Bogda Mountain, Xinjiang, Northwestern China since the Late Mesozoic: *Acta Geologica Sinica*, v. 81, p. 1507–1517. In Chinese with English abstract
- Wang, B., Zhai, Y.Z., Kapp, P., de Jong, K., Zhong, L.L., Liu, H.S., Ma, Y.Z., Gong, H.J., and Geng, H.Y., 2018b, Accretionary tectonics of back-arc oceanic basins in the South Tianshan: Insights from structural, geochronological, and geochemical studies of the Wuwamen ophiolite mélange: *Geological Society of America Bulletin*, v. 130, no. 1–2, p. 284–306. [10.1130/B31397.1](https://doi.org/10.1130/B31397.1)
- Wang, Q., Zhang, P.Z., Freymueller, J.T., Bilham, R., Larson, K.M., Lai, X., You, X., Niu, Z., Wu, J., Li, Y., Liu, J., Yang, Z., and Chen, Q., 2001, Present-day crustal deformation in China constrained by global positioning system measurements: *Science*, v. 294, no. 5542, p. 574–577. [10.1126/science.1063647](https://doi.org/10.1126/science.1063647)
- Wartes, M.A., Carroll, A.R., and Greene, T.J., 2002, Permian sedimentary record of the Turpan-Hami basin and adjacent regions, northwest China: Constraints on post-amalgamation tectonic evolution: *Geological Society of America Bulletin*, v. 114, no. 2, p. 131–152. [10.1130/0016-7606\(2002\)114<0131:PSROTT>2.0.CO;2](https://doi.org/10.1130/0016-7606(2002)114<0131:PSROTT>2.0.CO;2)
- Wilhem, C., Windley, B.F., and Stampfli, G.M., 2012, The Altaids of Central Asia: A tectonic and evolutionary innovative review: *Earth-Science Reviews*, v. 113, p. 303–341. [10.1016/j.earscirev.2012.04.001](https://doi.org/10.1016/j.earscirev.2012.04.001)
- Windley, B.F., Alexeev, D., Xiao, W.J., Kröner, A., and Badarch, G., 2007, Tectonic models for accretion of the Central Asian Orogenic Belt: *Journal of the Geological Society, London*, v. 164, no. 1, p. 31–47. [10.1144/0016-76492006-022](https://doi.org/10.1144/0016-76492006-022)
- Wu, C.Y., Liu, J.M., He, X.H., Li, Z.G., and Zheng, W.J., 2022, Structural geometry of the Urumqi foreland thrust system, northern Tian Shan: Insights into the seismotectonics of the 2013 M 5.1 Urumqi earthquake and deformation pattern in the Urumqi area: *Tectonophysics*, v. v, p. 829, 229294. [10.1016/j.tecto.2022.229294](https://doi.org/10.1016/j.tecto.2022.229294)
- Wu, C.Y., Ren, G.X., Wang, S.Y., Yang, X., Chen, G., Duan, L., Zhang, Z.Q., Zheng, W.J., Li, C.Y., Ren, Z.K., Lei, Q.Y., and Zhang, D.L., 2021, Late Quaternary active faulting on the inherited Baoer tu basement fault within the eastern Tian Shan orogenic belt: Implications for regional tectonic deformation and slip partitioning, NW China: *Geological Society of America Bulletin*, p. B35887. [10.1130/B35887.1](https://doi.org/10.1130/B35887.1)
- Wu, C.Y., Wu, G.D., Shen, J., Dai, X.Y., Chen, J.B., and Song, H.P., 2016, Late Quaternary tectonic activity and crustal shortening rate of the Bogda mountain area, eastern Tian Shan, China: *Journal of Asian Earth Sciences*, v. 119, p. 20–29. [10.1016/j.jseas.2016.01.001](https://doi.org/10.1016/j.jseas.2016.01.001)
- XBGMR (Xinjiang Bureau of Geology and Mineral Resources), 1965 v. 1, p. 200,000. Geological map, Urumqi sheet (K-45-IV)
- XBGMR (Xinjiang Bureau of Geology and Mineral Resources), 1978 , v. 1 , p. 200,00. Geological map, Turpan sheet (K-45-XII)
- XBGMR (Xinjiang Bureau of Geology and Mineral Resources), 1993, Regional Geology of Xinjiang Uygur Autonomy Region, Geology Publishing House, Beijing, p. 841. in Chinese
- Xiao, W., Han, C., Yuan, C., Sun, M., Lin, S., Chen, H., Li, Z., Li, J., and Sun, S., 2008, Middle Cambrian to Permian subduction-related accretionary orogenesis of Northern Xinjiang, NW China: Implications for the tectonic evolution of Central Asia: *Journal of Asian Earth Sciences*, v. 32, no. 2–4, p. 102–117. [10.1016/j.jseas.2007.10.008](https://doi.org/10.1016/j.jseas.2007.10.008)
- Xiao, W.J., Windley, B.F., Allen, M.B., and Han, C.M., 2013, Paleozoic multiple accretionary and collisional tectonics of the Chinese Tianshan orogenic collage: *Gondwana Research*, v. 23, no. 4, p. 1316–1341. [10.1016/j.gr.2012.01.012](https://doi.org/10.1016/j.gr.2012.01.012)
- Xiao, W.J., Windley, B.F., Yuan, C., Sun, M., Han, C.M., Lin, S.F., Chen, H.L., Yan, Q.R., Liu, D.Y., Qin, K.Z., Li, J.L., and Sun, S., 2009, Paleozoic multiple subduction-accretion processes of the southern Altaids: *American Journal of Science*, v. 309, no. 3, p. 221–270. [10.2475/03.2009.02](https://doi.org/10.2475/03.2009.02)
- Xiao, W.J., Zhang, L.C., Qin, K.Z., Sun, S., and Li, J.L., 2004, Paleozoic accretionary and collisional tectonics of the Eastern Tianshan (China): Implications for the continental growth of Central Asia: *American Journal of Science*, v. 304, no. 4, p. 370–395. [10.2475/ajs.304.4.370](https://doi.org/10.2475/ajs.304.4.370)
- Xie, W., Luo, Z.Y., Xu, Y.G., Chen, Y.B., Hong, L.B., Ma, L., and Ma, Q., 2016a, Petrogenesis and geochemistry of the late Carboniferous rear-arc (or back-arc) pillow basaltic lava in the Bogda Mountains, Chinese North Tianshan: *Lithos*, v. 244, p. 30–42. [10.1016/j.lithos.2015.11.024](https://doi.org/10.1016/j.lithos.2015.11.024)
- Xie, W., Xu, Y.G., Luo, Z.Y., Chen, Y.B., Liu, H.Q., Hong, L.B., and Ma, L., 2016b, Petrogenesis and geodynamic implications of the late Carboniferous felsic volcanics in the Bogda belt, Chinese Northern Tianshan: *Gondwana Research*, v. 39, p. 165–179. [10.1016/j.gr.2016.07.005](https://doi.org/10.1016/j.gr.2016.07.005)
- XIGMR (Xi'an Institute of Geology and Mineral Resources), 2007, Chinese Tianshan and its Adjacent Area 1:1 000,000, in Centre, X.A.G.S. (Ed.), Geological Publishing House, Beijing.
- Yang, Y.T., Guo, Z.X., and Luo, Y.J., 2017, Middle-Late Jurassic tectonostratigraphic evolution of Central Asia, implications for the collision of the Karakoram-Lhasa Block with Asia: *Earth-Science Reviews*, v. 166, p. 83–110. [10.1016/j.earscirev.2017.01.005](https://doi.org/10.1016/j.earscirev.2017.01.005)

- Yin, J.Y., Chen, W., Hodges, K.V., Xiao, W.J., Cai, K.D., Yuan, C., Sun, M., Liu, L.P., and van Soest, M.C., 2018, The thermal evolution of Chinese central Tianshan and its implications: Insights from multi-method chronometry: *Tectonophysics*, v. 722, p. 536–548. Doi:[10.1016/j.tecto.2017.11.037](https://doi.org/10.1016/j.tecto.2017.11.037)
- Yin, A., Nie, S., Craig, P., Harrison, T.M., Ryerson, F.J., Xianglin, Q., and Geng, Y., 1998, Late Cenozoic tectonic evolution of the southern Chinese Tian Shan: *Tectonics*, v. 17, no. 1, p. 1–27. Doi:[10.1029/97TC03140](https://doi.org/10.1029/97TC03140)
- Zhang, Y., Li, Z.S., Nie, F., Tian, X.L., and Shi, Y.H., 2015, Age, provenance and tectonic evolution of Late Paleozoic strata in Bogda Mountain, Xinjiang: Evidence from detrital zircon U-Pb geochronology: *Chinese Journal of Geology*, v. 50, no. 1, p. 155–181. in Chinese with English abstract
- Zhang, X., Zhao, G., Sun, M., Eizenhöfer, P.R., Han, Y., Hou, W., Liu, D., Wang, B., Liu, Q., and Xu, B., 2016, Tectonic evolution from subduction to arc-continent collision of the Junggar ocean: Constraints from U-Pb dating and Hf isotopes of detrital zircons from the North Tianshan belt, NW China: *Geological Society of America Bulletin*, v. 128, no. 3–4, p. 644–660. Doi:[10.1130/B31230.1](https://doi.org/10.1130/B31230.1)
- Zhao, X., Xue, C., Zhao, W., Seltmann, R., Symons, D.T.A., Dolgopolova, A., and Zhang, Y., 2021, Cooling and exhumation of the Late Paleozoic Tulasu epithermal gold system, Western Tianshan, NW China: Implications for preservation of Pre-Mesozoic epithermal deposits: *Journal of the Geological Society*, v. 178, no. 2, p. jgs2020–099. Doi:[10.1144/jgs2020-099](https://doi.org/10.1144/jgs2020-099)
- Zhong, L.L., Wang, B., de Jong, K., Zhai, Y.Z., and Liu, H.S., 2019, Deformed continental arc sequences in the south Tianshan: New constraints on the early Paleozoic accretionary tectonics of the Central Asian Orogenic Belt: *Tectonophysics*, v. 768, p. 228169. Doi:[10.1016/j.tecto.2019.228169](https://doi.org/10.1016/j.tecto.2019.228169)
- Zhong, L.L., Wang, B., Shu, L., Liu, H., Mu, L., Ma, Y., and Zhai, Y., 2015, Structural overprints of early Paleozoic arc-related intrusive rocks in the Chinese Central Tianshan: Implications for Paleozoic accretionary tectonics in SW Central Asian Orogenic Belts: *Journal of Asian Earth Science*, v. 113, p. 194–217. Doi:[10.1016/j.jseas.2014.12.003](https://doi.org/10.1016/j.jseas.2014.12.003)
- Zhu, Y.F., Guo, X., Song, B., Zhang, L.F., and Gu, L.B., 2009, Petrology, Sr-Nd-Hf isotopic geochemistry and zircon chronology of the Late Palaeozoic volcanic rocks in the southwestern Tianshan Mountains, Xinjiang, NW China: *Journal of Geological Society*, v. 166, no. 6, p. 1085–1099. Doi:[10.1144/0016-76492008-130](https://doi.org/10.1144/0016-76492008-130)
- Zhu, W.B., Shu, L.S., Sun, Y., Wang, F., and Zhao, Z.Y., 2006, Mesozoic-Cenozoic Deformation of the Central Structure Belt in the Turpan-Hami Basin, Northwest China: Tectonic Evolution of an Intracontinental Basin, Central Asia: *International Geology Review*, v. 48, no. 3, p. 271–285. Doi:[10.2747/0020-6814.48.3.271](https://doi.org/10.2747/0020-6814.48.3.271)
- Zhu, X.Y., Wang, B., Cluzel, D., He, Z.Y., Zhou, Y., and Zhong, L.L., 2019, Early Neoproterozoic gneissic granitoids in the southern Yili Block (NW China): Constraints on microcontinent provenance and assembly in the SW Central Asian Orogenic Belt: *Precambrian Research*, v. 325, p. 111–131. Doi:[10.1016/j.precamres.2019.02.019](https://doi.org/10.1016/j.precamres.2019.02.019)
- Zhu, W.B., Wan, J.L., Shu, L.S., Sun, Y., and Wang, F., 2004, Mesozoic-Cenozoic thermal history of TurpanHami Basin: Apatite fission track constrains: *Progress in Natural Science*, v. 15, no. 4, p. 331–336. in Chinese. Doi:[10.1002070512331342190](https://doi.org/10.1002070512331342190)